Wang *et al. Chem Synth* 2024;4:29
DOI: 10.20517/cs.2023.61

Chemical Synthesis

Review

Open Access

Check for updates

Advancements and applications of three-dimensional covalent organic frameworks

Rui Wang[1,#], Jie Zhao[2,#], Qianrong Fang[1,*], Shilun Qiu[1]

[1]State Key Laboratory of Inorganic Synthesis and Preparative Chemistry, Jilin University, Changchun 130012, Jilin, China.
[2]SINOPEC Research Institute of Petroleum Processing, Beijing 100083, China.
[#]Authors contributed equally.

[*]**Correspondence to:** Prof. Qianrong Fang, State Key Laboratory of Inorganic Synthesis and Preparative Chemistry, Jilin University, No.2699 Qianjin Street, Changchun 130012, Jilin, China. E-mail: qrfang@jlu.edu.cn

How to cite this article: Wang R, Zhao J, Fang Q, Qiu S. Advancements and applications of three-dimensional covalent organic frameworks. *Chem Synth* 2024;4:29. https://dx.doi.org/10.20517/cs.2023.61

Received: 1 Dec 2023 **First Decision:** 30 Jan 2024 **Revised:** 6 Feb 2024 **Accepted:** 29 Feb 2024 **Published:** 31 May 2024

Academic Editor: Xiang-Dong Yao **Copy Editor:** Pei-Yun Wang **Production Editor:** Pei-Yun Wang

Abstract

Covalent organic frameworks (COFs) represent an emerging class of crystalline porous polymers characterized by their pre-designed interconnected structures formed via dynamic covalent bonds. These materials have garnered widespread attention in recent years. While applications of two-dimensional (2D) COFs have been extensively investigated since 2005, their practicality has been impeded by their limited specific surface area and the robust π-π stacking interaction. In contrast, three-dimensional (3D) COFs boast enhanced porosity, larger specific surface area, well-exposed functional groups, and an abundance of reaction sites, positioning them at the forefront of porous material research. They find extensive applications in diverse fields, including adsorption, separation, catalysis, and so on. This featured article provides a comprehensive exploration of the latest advancements in 3D COFs across their respective application domains. Additionally, we outline the current challenges that must be addressed and shed light on the promising prospects for the utilization of 3D COFs.

Keywords: Covalent organic frameworks, application, crystalline porous materials, functionalization

INTRODUCTION

Covalent organic frameworks (COFs) represent an emerging class of constant and porous crystalline polymers intricately woven together by multifunctional organic building units[1]. In 2007, El-Kaderi *et al.* pioneered the design of a groundbreaking three-dimensional (3D) porous COF by interconnecting pre-

designed organic building blocks[2]. Subsequently, researchers have embarked on developing new 3D COFs using various organic building units and conducting comprehensive investigations into their applications[3]. What is particularly intriguing is that when compared to two-dimensional (2D) counterparts, 3D COFs boast higher surface areas, uniform interpenetrating channels, and a greater number of exposed active sites, rendering them more competitive across various application fields[4]. Furthermore, 3D COFs with precisely defined crystal structures can be functionalized through a multitude of methods, making them an ideal platform for research focused on structural regulation and the elucidation of structure-function relationships[5].

However, despite the great potential of 3D COFs in various application fields, the literature on their applications remains limited (less than 200 reported studies)[6]. This limitation stems from several factors. Firstly, the absence of π-π stacking interactions and the presence of large internal void spaces pose significant challenges in crystallizing 3D COF structures[7]. Additionally, the topologies and conformations of 3D COFs can vary considerably, making their structures challenging to elucidate. The limited availability of diverse 3D organic building blocks, coupled with their inherent instability, further restricts the range of synthesizable 3D COFs[8]. Furthermore, these frameworks typically exhibit small pore sizes and even incorporate interpenetrating channels. This complexity makes their functionalization through post-modification methods more challenging[9]. Consequently, they currently find application in only a handful of specific areas, such as gas storage, separation, chemical sensing, catalysis, batteries, and so on[10]. For example, El-Kaderi *et al.* first used 3D COFs for gas adsorption in 2007[2]. Fang *et al.* employed them for catalysis for the first time in 2014[11].

In addition, the thermal stability of 3D COFs exceeds that of 2D COFs characterized solely by π-π stacking, thanks to their intrinsic interpenetrating structure. Recent studies have emphasized the influence of linker types on the thermal stability of 2D COFs[12]. Specifically, borate-linked COFs exhibit superior thermal stability compared to their imine-linked counterparts. Simultaneously, networks with smaller pores demonstrate enhanced thermal stability than those with larger pores. Additionally, functionalized COFs generally exhibit lower thermal stability than non-functionalized ones. While these findings have not been explicitly validated in the context of 3D COFs, they provide valuable insights for reference.

In spite of these challenges, 3D COFs continue to stand as an appealing platform for further applications owing to their distinctive properties and ability to provide intricately designed pore structures[13]. Furthermore, they feature an abundance of void spaces, resulting in a larger surface area and readily accessible active sites, greatly benefiting practical applications[14]. Surprisingly, over the past decade, while numerous reviews have discussed the applications of 2D COFs, there has been limited exploration of the potential applications of 3D COFs[15]. This review seeks to comprehensively introduce all reported applications of 3D COFs across various fields and delineate the current challenges and prospects for expanding the utilization of 3D COFs.

DESIGN AND SYNTHESIS OF 3D COFS

Features of 3D COFs

In comparison to 2D COFs, 3D COFs exhibit unique characteristics that amplify their versatility across diverse applications. A prominent attribute is the presence of interpenetrating channels in 3D COFs, a feature absent in their 2D counterparts[5]. These channels not only fortify the stability of 3D COFs but also further diminish pore size[16]. Recent reports suggest that the degree of interpenetration in these channels can be regulated to some extent[17]. Additionally, the specific surface area of 3D COFs significantly surpasses that of 2D COFs, with numerous 3D COF materials reporting specific surface areas exceeding 2,000 $m^2 \cdot g^{-2}$ -

a rarity in 2D COFs[18]. Furthermore, 3D COFs exhibit lower densities, exemplified by JUC-640-H, boasting a density of only 0.106 $cm^3 \cdot g^{-1}$, the highest among crystalline materials[19]. This heightened specific surface area facilitates the exposure of more functional groups within the pores, promoting not only the post-functionalization of COFs but also expanding their applications in catalytic energy storage and other fields.

Topology

Topology plays a pivotal role in the design of 3D COFs as it determines the size and distribution of pores within the 3D network[20]. Since the pioneering report by El-Kaderi *et al.* in 2007, showcasing the first instance of a 3D COF, more than 20 new 3D topologies have been unveiled as shown in Scheme 1[2]. Among them, excluding eight specific ones - namely **srs**[21], **fjh**[22], **she**[23], **ffc**[24], **tbo**[25], **pto**[26], **mhq-z**[26], and **nbo**[27] - all others incorporate spatial building blocks. Tetrahedral building blocks are the most prevalent spatial construction units, encompassing examples such as **dia**[28], **pts**[29], **ctn**[2], **bor**[2], **qtz**[30], **lon-b**[31] and **ljh**[32]. Alongside tetrahedral blocks, triptycene building blocks are also commonly employed in the creation of 3D COFs, resulting in successful topologies such as **stp**[33], **acs**[34], **ceq**[34,35] and **hea**[36]. Recently, eight-node building blocks have also been harnessed to craft new topologies, such as **bcu**[37], **pcb**[38], **flu**[39], **scu**[40] and **tty**[41]. Beyond the common building blocks mentioned previously, unique monomers are utilized to fashion distinctive topologies. For instance, **rra**[42] is derived from γ-cyclodextrins, the **pcu**[43] topology is constructed from triangular antitriangular prisms, and **soc**[44] topologies encompass building units generated through octahedral titanium coordination. The development of novel spatial building blocks and their creative amalgamation with existing ones stands as an effective strategy for generating fresh topologies in the realm of 3D COFs.

Linkage

Linkage is a fundamental requirement for the construction of COFs. Traditionally, COF linkers have been known for their rigidity and dynamism. However, as research has advanced, some less reversible linkages have also been applied in COF synthesis[3]. It is important to note that while new linkages have been reported in the realm of 2D COFs, not all of them seamlessly translate to the fabrication of 3D COFs[45]. This limitation often arises from the need to distort certain linkages to conform to the spatial configuration of 3D COFs. Scheme 2 illustrates the successful incorporation of linkages in 3D COFs, including boryl-based linkages such as boroxine[2], boronate ester[2], spiroborate[35] and borosilicate[46], along with nitrile-based linkages such as imine[28], amide[47], imide[48], trazine[49] and azodioxy[50]. Additionally, there have been instances where 3D COFs were ingeniously constructed using two distinct linkages. In addition to the previously mentioned bond types, other robust covalent bonds, such as olefins[51] and β-ketoenamines[52], have been developed to enhance the stability of 3D COFs.

Synthesis

While numerous methods are available for synthesizing 2D COFs, only a select few, such as solvothermal heating, ionic heating, microwave synthesis, ultrasonic-assisted techniques, and plasma-induced methods, have successfully been adapted for the production of 3D COFs[53]. To date, the vast majority of 3D COFs have been synthesized using solvothermal methods[3]. Given the diverse building blocks chosen for COFs, various parameters of solvothermal synthesis, including solvent choice, temperature, catalyst, reaction time, and more, must be meticulously explored. In addition to solvothermal techniques, ionic thermography has garnered attention from researchers due to its gentle synthesis conditions and rapid reaction times[54]. In this approach, ionic liquids serve as both solvents and catalysts for COF synthesis, enabling the swift production of COFs at ambient temperatures.

Microwave synthesis and ultrasonic-assisted synthesis have recently garnered significant attention as alternative methods for synthesizing COFs compared to traditional solvothermal heat. Among these, the

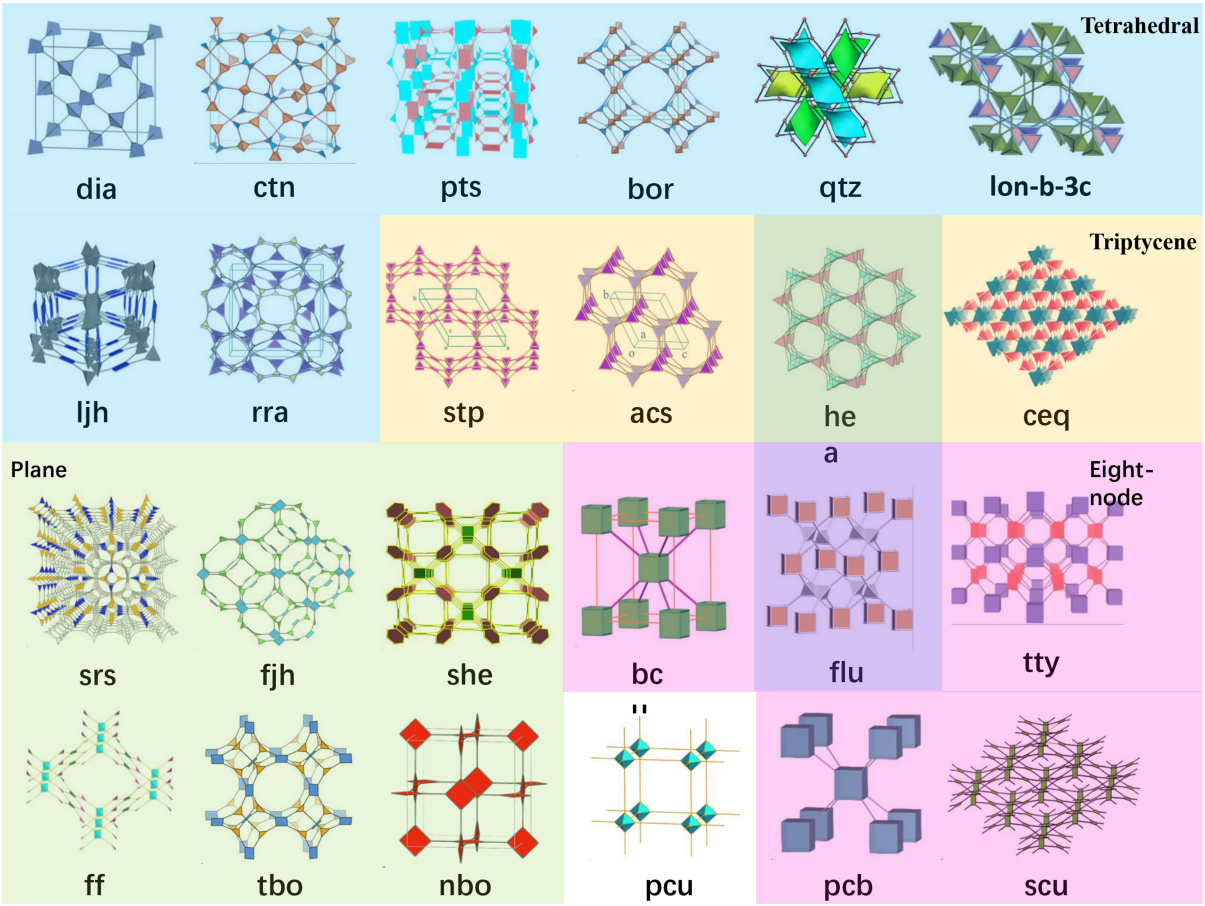

Scheme 1. Topologies in 3D COFs. 3D: Three-dimensional; COFs: covalent organic frameworks.

microwave method typically employs microwave radiation in the range of 1 mm to 1 m[55], generated by a microwave reactor, and finds widespread application in organic synthesis. Despite the relatively low energy of microwaves, insufficient for breaking most chemical bonds, the high-frequency electric field accompanying microwaves compels molecules or ions in the reaction mixture to lose energy through collisions, leading to efficient internal heating[56]. Consequently, the efficiency of heat energy absorption by molecules exceeds that of traditional ovens and oil baths, markedly reducing reaction time and potentially enhancing COF yield and crystallinity. Leveraging the unique properties of microwave synthesis, it may hold substantial application value in COF synthesis, akin to organic synthesis. Microwave synthesis, first reported by Campbell *et al.* in 2009, offers a significantly shorter reaction time compared to traditional solvothermal methods while preserving the crystallinity and specific surface area of COFs[57].

The ultrasonic synthesis method utilizes ultrasonic waves in the frequency range of 20 kHz to 1 MHz to generate bubbles and collapses in a liquid medium[58]. Although the energy of ultrasound is weak and insufficient for altering the vibration or spin state of electrons in atoms, the moment of bubble formation or collapse may be accompanied by instantaneous heat or pressure, facilitating chemical reactions under these extreme conditions[59]. Zhao *et al.* recently first introduced an ultrasound-assisted synthesis method for 3D COFs in 2022[60].

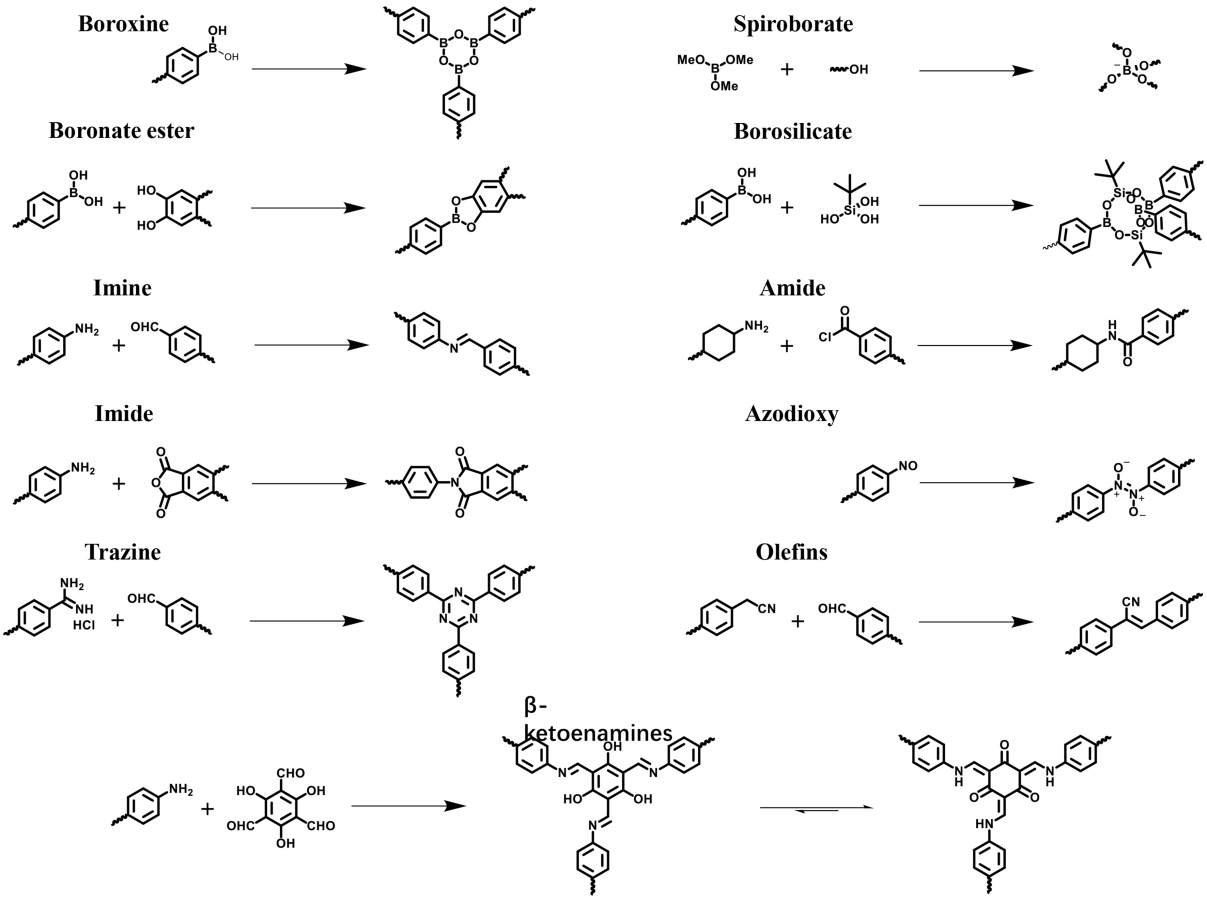

Scheme 2. Linkages in 3D COFs. 3D: Three-dimensional; COFs: covalent organic frameworks.

In 2021, He *et al.* developed a plasma-induced synthesis technique for 3D COFs, which boasts advantages such as low energy consumption, rapid synthesis, and no heating requirements, all while ensuring the crystallinity and high specific surface area of COFs[61]. In addition to polycrystalline synthesis methods, techniques for synthesizing 3D COF single crystals and films have also been developed. The first 3D single-crystal COF was reported by Beaudoin *et al.* in 2013,[50] while Zhang *et al.* reported a smaller single crystal linked by imine bonds around the same time[62]. In 2018, the same research group proposed a strategy for growing large-size (10-60 μm) 3D COF single crystals using aniline as a growth regulator[31]. In 2019, Evans prepared a series of 2D and 3D COF monocrystals via boroxine links, and colloidal suspension of COFs was stabilized with the addition of a co-solvent containing nitrile[63]. In 2022, Peng *et al.* demonstrated the rapid growth of large-size (110 μm) 3D COF single crystals at the millimeter level using supercritical carbon dioxide (CO_2) as a solvent[64]. Apart from single crystal synthesis, achieving 3D COF films poses equally significant challenges. The first 3D COF membrane was grown *in situ* by Lu *et al.* on an α-Al_2O_3 substrate[65], and a similar approach was adopted by Fu *et al.* on a polyaniline-modified silicon substrate[66]. More recently, Yang *et al.* successfully synthesized an ultra-thin (13 nm) 3D COF crystal film using a two-phase interface method, enabling production at a centimeter scale[67].

Functionalization of 3D COFs

Generally, three strategies are employed for COF functionalization. The first entails pre-modifying functional groups on the monomers before using these functionalized monomers to synthesize COFs. This method ensures enough COF functional groups with predetermined positions and distributions, thereby

enhancing material properties. However, challenges in crystallization and a reduction in specific surface area may arise due to spatial hindrance during COF synthesis on the monomer side chain[68]. The second method involves pre-synthesizing COFs while retaining some functional groups on the side chain for further reactions. COFs with these functional groups can react with monomeric small molecules and undergo modifications on the side chains. This approach preserves high COF crystallinity but may lead to lower functionalization degrees and diminished material performance. Ensuring chemical stability during further reactions is crucial for the COF framework in this method. It is important to note that active sites may not be uniformly distributed, and the modification amount may be uncontrollable, hindering the construction of structure-activity relationships. Several mild covalent transformations for 3D COF modifications have been explored, including thiol-alkene coupling reactions, copper-mediated azide-alkyne cycloaddition, and ring-opening reactions. For instance, Bunck and Dichtel reported the first example of 3D COF modification based on a 3D boroxane-linked COF-102-allyl group[69]. The last method of functionalizing COFs involves intrinsically introducing functionalized substances into COFs, such as *in-situ* growth of metal nanoparticles or composite materials achieving COF growth on other materials (e.g., graphene or MXene)[70]. *Ex-situ* methods can also be employed to introduce functionalized metal ions or non-metallic particles into COF pores. This approach uses COF as a carrier, ensuring uniform dispersion of functionalized substances, preventing agglomeration, and preserving performance[71]. However, this method is closely tied to COF porosity and its ability to interact with functionalized substances. Additionally, due to the uncertainty of modification, understanding the structure-activity relationship becomes challenging.

APPLICATIONS OF 3D COFS

Uptake, storage and separation

Capture and adsorption of carbon dioxide

CO_2 is a major greenhouse gas and a potential carbon source, making its capture a key environmental concern[72]. Additionally, 3D COFs have emerged as ideal platforms for capturing CO_2, offering potential solutions to mitigate the issues associated with the greenhouse effect[73]. In 2009, Furukawa *et al.* designed two novel 3D COFs, COF-102 and COF-103, and for the first time, measured their CO_2 capture capacities[74]. COF-102 exhibited a high CO_2 capacity of 1,200 mg·g^{-1}, while COF-103 reached 1,190 mg·g^{-1} at 298 K and 55 bar, surpassing the performance of 2D COFs, which typically do not exceed 1,010 mg·g^{-1}. Furthermore, research by Li *et al.* introduced 3D COFs with two types of covalent linkages as shown in Figure 1A and B. DL-COF-1 and DL-COF-2 demonstrated CO_2 uptake capacities of 136 and 111 cm^3·g^{-1}, respectively, at 273 K and 1 bar[75]. This group also developed metal-free 3D ionic COFs, 3D-ionic-COF-1 and 3D-ionic-COF-2, with CO_2 capacities of 161 mg·g^{-1} at 273 K and 93 mg·g^{-1} at 298 K for 3D-ionic-COF-1, and 133 mg·g^{-1} at 273 K and 76 mg·g^{-1} at 298 K for 3D-ionic-COF-2[76]. Additionally, Guan *et al.* identified a novel 3D azine-linked COF, 3D-HNU5, with excellent CO_2 uptake performance, achieving a capacity of 123.1 mg·g^{-1} at 273 K[77]. In 2020, Zhu *et al.* synthesized the first 3D organic cage COF, named 3D-CageCOF-1, which exhibited a CO_2 uptake of 204 mg·g^{-1} at 273 K and 1 bar, and 107 mg·g^{-1} at 298 K and 1 bar[78]. Moreover, research by Kumar *et al.* resulted in a **dia** network that instigated a nine-fold interpenetration imine-based 3D COF in 2020, containing 2,2'-bipyridyl units. This structure demonstrated a CO_2 uptake capacity of 88.35 cm^3·g^{-1} at 273 K and 61.5 cm^3·g^{-1} at 298 K[79]. On the other hand, Li *et al.* designed a novel two-fold interpenetrated **ceq** topology 3D COF with a CO_2 uptake capacity reaching 179 mg·g^{-1} at 273 K[35]. Gao *et al.* synthesized three isostructural 3D-TPB-COFs, each exhibiting a high CO_2 uptake: 3D-TPB-COF-H (180 mg·g^{-1}), 3D-TPB-COF-F (182 mg·g^{-1}), and 3D-TPB-COF-Me (174 mg·g^{-1})[80]. Lin *et al.* reported a novel 3D pyrene-based COF with a CO_2 capture capacity of 139.6 mg·g^{-1}[29]. In 2021, Li *et al.* designed and synthesized two 3D triptycene-based COFs, named JUC-568 and JUC-569, with non-interpenetrated **acs** or **ceq** topology. Notably, JUC-568 exhibited impressive CO_2 uptake performance, with 98 cm^3·g^{-1} at 273 K and 1 bar[34]. The same group reported two 3D COFs with **hea** topology the following year, achieving CO_2 adsorption capacities of 84 cm^3·g^{-1} at 273 K and 53 cm^3·g^{-1} at 298 K for JUC-596, and

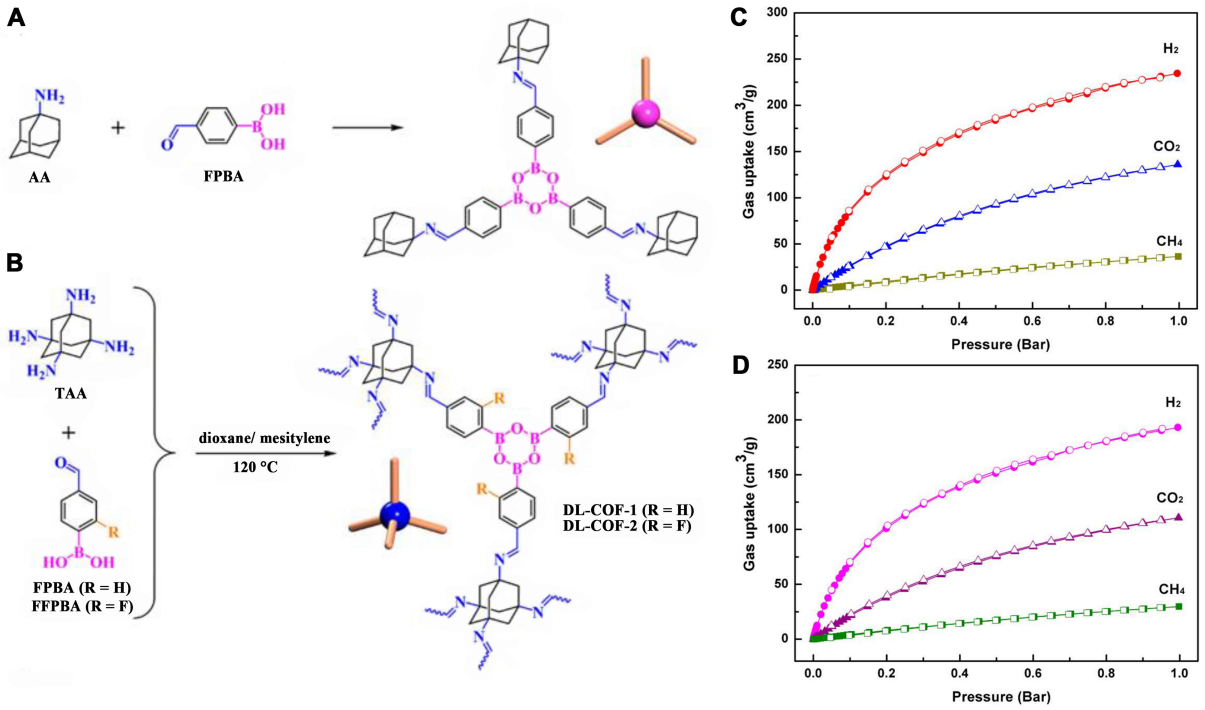

Figure 1. (A and B) Schematic diagram of Preparing DL-COFs structures with dual for gas adsorption; (C) Adsorption isotherms for H_2, CO_2, and CH_4 on DL-COF-1; (D) DL-COF-2. Reproduced from ref[75], with permission from the American Chemical Society, Copyright 2016. COFs: Covalent organic frameworks.

70 $cm^3 \cdot g^{-1}$ at 273 K and 31 $cm^3 \cdot g^{-1}$ at 298 K for JUC-597[36]. Furthermore, Zhu *et al.* designed several 3D COFs with **pto** and **mhq-z** topologies[26]. RICE-5 and RICE-7 exhibited CO_2 adsorption capacities of 50 $cm^3 \cdot g^{-1}$ and 24 $cm^3 \cdot g^{-1}$ at 1 bar, respectively. Zhang *et al.* constructed highly rigid 3D COFs through imine condensation, with CO_2 uptake capacities of 1.1 and 1.83 $mmol \cdot g^{-1}$ at 298 K and 100 kPa for SP-CA-COF-IM and SP-CA-COF-AM, respectively[81]. Song *et al.* successfully synthesized a new microporous COF named JUC-610 through [4 + 4] imine condensation reactions, displaying a high CO_2 uptake of 45 $cm^3 \cdot g^{-1}$ at 273 K and 1 bar[82].

Adsorption and storage of hydrogen

Air pollution and global warming have become significant challenges confronting humanity, necessitating the proactive pursuit of clean energy and storage solutions[83]. Hydrogen (H_2) energy has garnered considerable attention as a promising green energy source[84]. However, it presents substantial challenges in terms of transportation and storage[85]. Characterized by their exceptionally high surface area, well-defined structures, and abundant open 3D channels, 3D COFs emerge as ideal candidates for H_2 storage[86]. In 2009, Furukawa and Yaghi conducted measurements of H_2 storage capacity for both 2D and 3D COFs[74]. Intriguingly, 3D COFs, specifically COF-102 and COF-103, exhibited remarkable saturation H_2 uptake values of 72.4 and 70.5 $mg \cdot g^{-1}$ at 77 K and 35 bar, respectively. This underscores the distinct advantages of 3D COFs over their 2D counterparts. In 2012, Kalidindi *et al.* successfully integrated palladium (Pd) nanoparticles into COF-102, resulting in a more than two-fold enhancement in H_2 storage capacity at room temperature and 20 bar[87]. However, Campbell *et al.* synthesized COF-102 using a mild microwave thermal method, yielding a disappointingly low hydrogen uptake of less than 1.7 wt% at 1 bar and 77.3 K[57]. Meanwhile, the DL-COF, prepared by Li *et al.*, exhibited H_2 storage capacities of 234 $cm^3 \cdot g^{-1}$ for DL-COF-1 and 193 $cm^3 \cdot g^{-1}$ for DL-COF-2 at 77 K and 1 bar [Figure 1C][75]. Similar excellent performances were shown

by JUC-568 and JUC-569, in which JUC-568, in particular, demonstrated an impressive hydrogen uptake of 274 $cm^3 \cdot g^{-1}$ at 77 K and 1 bar[34]. Furthermore, Yu *et al.* designed JUC-596 with a **hea** topology, showcasing exceptional performance in H_2 adsorption, reaching an impressive 2.72 wt% (305 $cm^3 \cdot g^{-1}$) at 77 K and 1 bar[36]. This accomplishment positions JUC-596 among the best porous organic materials for H_2 storage reported to date. In the same year, Li *et al.* reported similar findings[88]. Additionally, Liao *et al.* designed two 3D imine-based COFs featuring rare bcu nets, named JUC-588 and JUC-589, which exhibited H_2 uptake capacities of 245 and 211 $cm^3 \cdot g^{-1}$, respectively, at 77 K and 1 bar[89].

Capture and adsorption of methane

Methane (CH_4) is considered a relatively clean energy carrier and is being explored as a potential alternative to oil due to increasing demand and its potential to reduce carbon emissions[90]. However, CH_4 also has a significant drawback - its low energy density and its classification as a greenhouse gas[91]. As a result, there has been a surge in research focused on developing effective materials for CH_4 adsorption[92]. Additionally, 3D COFs have garnered significant attention as promising candidates for CH_4 storage[1]. This is primarily due to their low density, large surface area, and substantial void spaces. However, research in this field remains relatively limited[2-5]. A groundbreaking study for the CH_4 adsorption by 3D COFs was demonstrated, measured under various conditions. Furukawa *et al.* investigated two 3D COFs, namely COF-102 and COF-103[74]. Notably, at 298 K and 35 bar, COF-102 exhibited exceptional CH_4 adsorption capacity, reaching 187 $mg \cdot g^{-1}$, while COF-103 achieved 175 $mg \cdot g^{-1}$. Even under increased pressure at 85 bar, COF-102 maintained robust performance with an adsorption capacity of 243 $mg \cdot g^{-1}$, while COF-103 reached 229 $mg \cdot g^{-1}$. Meanwhile, Ma *et al.* achieved a notable breakthrough by successfully synthesizing a novel 3D Metal-Covalent Organic Frameworks (MCOF) named MCOF-1[93]. Under standard conditions of 298 K and 1 bar, MCOF-1 displayed impressive adsorption capacities for various gases, including CH_4 (9 $mL \cdot g^{-1}$), C_2H_4 (36 $mL \cdot g^{-1}$), C_2H_6 (44 $mL \cdot g^{-1}$), and C_3H_8 (55 $mL \cdot g^{-1}$). Both DL-COF-1 and DL-COF-2 exhibited substantial CH_4 adsorption capacities at 273 K and 1 bar, specifically 36 and 30 $mL \cdot g^{-1}$ [Figure 1C][75]. These materials exhibited substantial CH_4 adsorption capacities at 273 K and 1 bar, specifically 36 and 30 $mL \cdot g^{-1}$ [Figure 1D]. Similarly, both JUC-568 and JUC-569 have also been explored for CH_4 adsorption[34]. JUC-568 demonstrated higher CH_4 adsorption capacity at 273 and 298 K, reaching 48 and 32 $mL \cdot g^{-1}$, respectively, in comparison to JUC-569, which achieved 19 $mL \cdot g^{-1}$ at 273 K and 11 $mL \cdot g^{-1}$ at 298 K. Furthermore, the same research group introduced a novel triptycene-based **hea** topology in 2022, and they investigated the CH_4 adsorption performance of both 3D COFs. Likewise, the triptycene-based 3D COFs (JUC-596 and JUC-597) are also promising for CH_4 adsorber exhibiting a maximum adsorption capacity of 31 $mL \cdot g^{-1}$ at 273 K and 14 $mL \cdot g^{-1}$ at 298 K for JUC-596, while JUC-597 achieved 25 $mL \cdot g^{-1}$ at 273 K and 8 $mL \cdot g^{-1}$ at 298 K[36]. In 2022, Li *et al.* reported similar outcomes[88]. The same research team also reported the CH_4 adsorption performance of JUC-588 (16 $mL \cdot g^{-1}$) and JUC-589 (12 $mL \cdot g^{-1}$) at 273 K and 1 bar[89].

Capture of iodine

As global oil resources continue to deplete, nuclear energy has emerged as a green and environmentally friendly alternative that has garnered increasing attention over the years[94]. However, the presence of radioactive iodine isotopes (^{129}I and ^{131}I) in nuclear waste poses a major challenge[95]. These isotopes are known to sublimate easily into the gas phase, making them a significant source of radioactive vapor waste. Furthermore, they tend to dissolve readily in water, leading to adverse ecological consequences. Consequently, there has been a growing focus on finding efficient methods to capture and manage iodine in recent years[96]. In 2018, Wang *et al.* introduced a groundbreaking 3D COF (COF-DL229) characterized by a unique eight-fold interwoven diamond net structure, specifically designed for the purpose of removing iodine vapor. Impressively, this innovative material achieved an exceptional I_2 uptake capacity of 82.4 wt%[97]. Wang *et al.* devised a different approach by creating 3D tetrathiafulvalene (TTF)-1,3,5-tris(4-

aminophenyl)trianiline (TAPT)-COF with an **ffc** net, tailored to efficiently capture iodine vapor. This material demonstrated a remarkable I_2 adsorption capacity of 5.02 $g \cdot g^{-1}$[98]. As illustrated in Figure 2, Chang *et al.* delved into TTF-based 3D COFs, which displayed outstanding high I_2 adsorption capabilities, reaching levels as high as 8.19 $g \cdot g^{-1}$[99]. Moreover, these COFs exhibited rapid I_2 adsorption kinetics, clocking in at 0.70 $g \cdot g^{-1} \cdot h^{-1}$. These performance metrics significantly outshine those of other materials, including silver-doped adsorbents, and all known inorganic and organic porous materials. In 2023, Liu *et al.* achieved a milestone by developing 3D macro-microporous COF-300 single crystals designed specifically for iodine capture. This material showcased an impressive high adsorption capacity of 3.15 $g \cdot g^{-1}$[100]. In addition, Zou *et al.* synthesized diacetylene-based 3D COFs (CPOF-3), which proved to be highly effective adsorbents for iodine capture, exhibiting an outstanding adsorption capacity of up to 5.87 $g \cdot g^{-1}$[101]. These remarkable advancements represent significant progress in addressing the challenge of efficiently capturing and managing iodine from nuclear waste, offering promising solutions in the realm of nuclear waste management.

Extraction of ionic pollutants

As industrial processes develop, ion-containing wastewater with harmful environmental effects is inevitably generated during production[102]. How to effectively treat harmful ions in industrial wastewater and recover valuable metal ions from wastewater before discharge has become a recent research hotspot[103]. Furthermore, 3D COFs have the potential to adsorb ions due to their high specific surface area and the absence of any metallic elements[104]. Uranium is a crucial fuel for nuclear reactions, and when leaked into the environment, it poses significant health risks to humans[105]. Therefore, 3D COFs have also garnered widespread attention as adsorbents for uranium ions[106]. Cui *et al.* ingeniously designed a salen-functionalized 3D COF called tetrakis(4-aminophenyl)methane (TAPM)-3,3'-dihydroxy-[1,1'-biphenyl]-4,4'-dicarbaldehyde (DHBD) for concurrent UO_2^{2+} extraction, achieving a uranium extraction capacity of 955.3 $mg \cdot g^{-1}$[107]. In 2023, the same group designed a novel sp^2 carbon-linked 3D COF, named tetrakis(4-formylphenyl)methane (TFPM)-2,2'-(1,4-phenylene)diacetonitrile (PDAN)-amidoxime (AO), which serves as a platform for uranium extraction from seawater with an adsorption capacity of 4,685 $mg \cdot g^{-1}$[108]. Chen *et al.* constructed a 3D COF with hexameric binding sites for enhanced uranium adsorption capture, reaching up to 0.993 $mmol^{-1}$[109]. The enrichment of precious metals such as Au ions from seawater is also of great importance[110]. Liu *et al.* synthesized a new 3D COF named (3,3',5,5'-tetra(p-aminophenyl)-bimesitylene (BMTA)-TFPM-COF with a non-fold interpenetration **dia** topology for Au ion capture, which absorbs Au^{3+} with a high capacity of 570.18 $mg \cdot g^{-1}$ and selectivity of 99.5%[111]. Technetium ions are another class of harmful ions present in nuclear wastewater[112]. Zhang *et al.* reported an ionic sp^2 carbon-linked 3D COF with an adsorption capacity of 542.3 $mg \cdot g^{-1}$ for ReO_4^- ions (used as a substitute for TcO_4^-)[113]. Wang *et al.* reported a phosphonium-containing coating on 3D COF-g-VBPPh3Cl using a gamma ray pre-radiation approach, which can remove > 98% of ReO_4^- ions in a minute[114]. Li *et al.* developed a metal-free 3D ionic COF-2, with permanganate chosen as the model ion to substitute TcO_4^-, and almost 100% of MnO_4^- ions can be removed in less than 20 min[76]. In addition to radioactive ions, nuclear wastewater often contains fission products dominated by lanthanides, including Nd^{3+}, Sr^{2+}, and Fe^{3+}[115]. Another group reported a 3D COF in 2018 by postsynthetically modifying the 3D COF with carboxylic acids capable of capturing these three ions in water[116]. Among them, the ability to capture Nd^{3+} (15.87 M^{-1}) is much higher than that of Sr^{2+} (0.85 mM^{-1}) and Fe^{3+} (0.08 mM^{-1}). The removal of harmful ions, such as Hg^{2+} in water, is also an important application for COFs[117]. Zhang *et al.* reported 3D thioether-based COFs (JUC-570 and JUC-571) for Hg^{2+} removal for the first time[118]. The isopropyl groups around imine bonds on JUC-570 endow it with a high Hg^{2+} adsorption capacity (619 $mg \cdot g^{-1}$) at pH = 1.

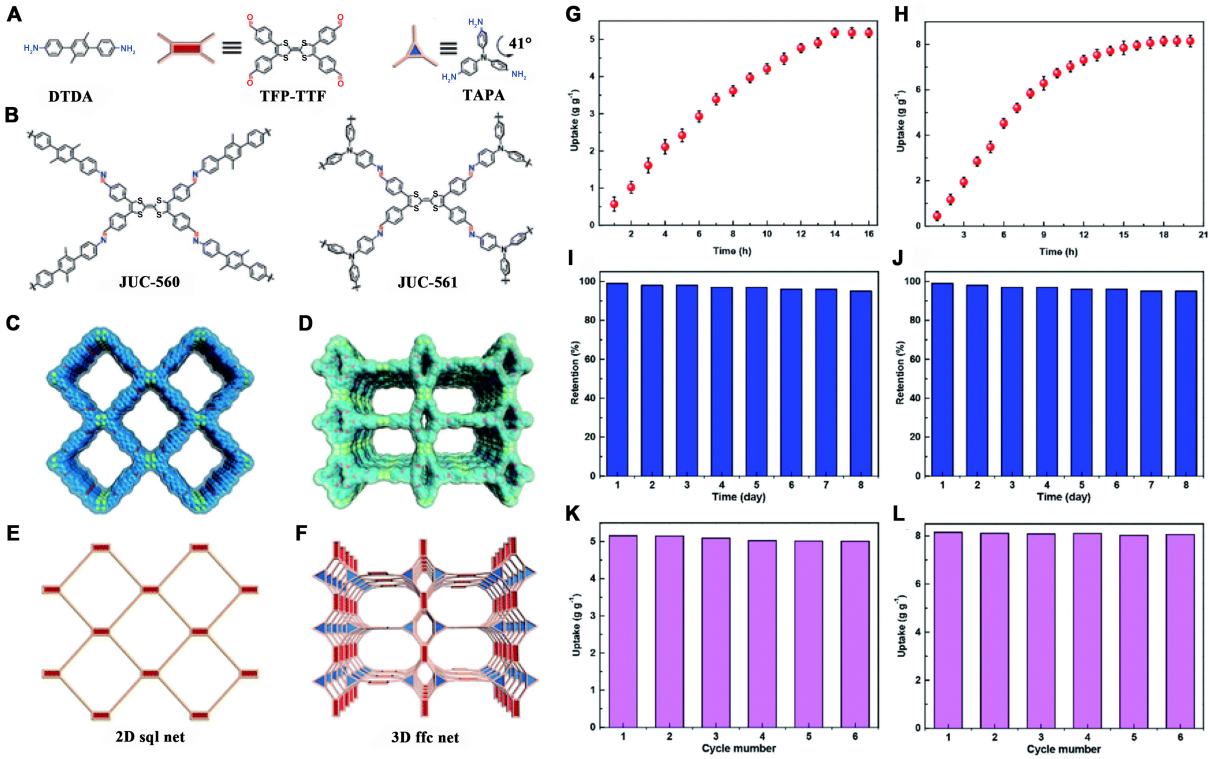

Figure 2. (A) Schematic diagram of the building unit structure of JUC-560 and JUC-561; (B) Schematic diagram of the structure of JUC-560 and JUC-561. Extended structures of mesoporous (C) 2D JUC-560 and (D) 3D JUC-561. 2D sql and 3D ffc net for (E) JUC-560 and (F) JUC-561 respectively; (G) Iodine uptake of JUC-560 as a function of exposure time at 75 °C and ambient pressure; (H) Iodine uptake of JUC-561 as a function of exposure time at 75 °C and ambient pressure; (I) Iodine retention of JUC-560 after capturing iodine upon exposure to air at 25 °C and ambient pressure; (J) Iodine retention of JUC-561 after capturing iodine upon exposure to air at 25 °C and ambient pressure; (K) Recyclability of JUC-560 in iodine adsorption; (L) Recyclability of JUC-561 in iodine adsorption. Reproduced with permission from ref[99], Copyright 2021, Royal Society of Chemistry. 2D: Two-dimensional; 3D: three-dimensional.

Capture of other organic carbon

Organic carbon capture, including the adsorption of organic vapors, dyes, pesticides, antibiotics, and other organic compounds, has only seen sporadic exploration regarding the application of 3D COFs[119]. Moroni *et al.* conducted research on the adsorption capacity of flexible imine COFs for benzene and cyclohexane[120]. Under conditions of 298 K and 1 bar, COF-300-rt, COF-300-st, and LZU-111 demonstrated higher adsorption capacities for benzene (251, 221, and 214 $cm^3 \cdot g^{-1}$) compared to cyclohexane (175, 133, and 164 $cm^3 \cdot g^{-1}$). Li *et al.* introduced a novel class of imine-linked 3D COFs with a boron-based topology, exhibiting exceptional adsorption capacity for benzene vapor (1,203.9 $mg \cdot g^{-1}$) at 298 K[121]. Mohammed *et al.* successfully demonstrated the application of a 3D-COF with cellulose acetate as a mixed-matrix membrane for removing over 80% of phenol from wastewater[122]. Lu *et al.* synthesized a 3D COF with a **dia** net structure, incorporating magnetic Fe_3O_4 for the uptake of bisphenol A (209.9 $mg \cdot g^{-1}$)[123]. The same research group developed an innovative 3D COF for selective solid-phase microextraction. Utilizing 3D 1,3,5-triformylphloroglucinol and tetra (p-aminophenyl) methane (TpTAM)-COF, they effectively extracted polychlorinated biphenyls from river water and soil, achieving removal rates of at least 84.8% and 84.4%, respectively[124]. In 2022, Li *et al.* harnessed 3D–OH–COF as a selective solid-phase microextraction agent, relying on hydrogen bonding interactions, to establish a high-performance liquid chromatography (HPLC) method for the simultaneous determination of acetamiprid, dimethipin, and amitrole in rice and apple samples[125]. Moreover, Li *et al.* unveiled the remarkable sorption capabilities of 3D COFs for ionic dyes. Specifically, 3D-ionic-COFs exhibited efficient adsorption of ionic dyes[76], with JUC-610 demonstrating a

high adsorption capacity for leucocrystal violet, achieving a removal rate of approximately 60% in just 100 min[82]. Additionally, JUC-589 effectively adsorbed dye molecules, including Coomassie brilliant blue R250[89]. In 2012, Bunck *et al.* reported on pristine COF-102 and dodecyl-functionalized COF-102-C12, both incorporating the solvatochromic dye pyridinium iodide[69]. The size of the pore size is also an important factor that restricts the adsorption capacity of porous materials with dyes[126]. Liu *et al.* explored the adsorption of three anionic fluorescent dyes within two 3D woven COFs (COF-506-Cu and COF-505-Cu), with results indicating a positive correlation between the size of the adsorbed dye and the inherent pore size of the COF[127].

Sustained release of drug

Sustained drug release is a pivotal strategy aimed at reducing dosing frequency and the overall drug dosage which helps maintain a stable drug concentration in the bloodstream, ultimately mitigating the toxic side effects of medications[128]. Fang *et al.* made a groundbreaking effort by designing and synthesizing the initial set of 3D polyimide COFs. They also embarked on using 3D COFs for controlled drug delivery for the first time [Figure 3][48]. During drug delivery, the 3D COFs exhibited a remarkable drug loading capacity and precise control over release rates. In 2022, the same research group achieved another milestone, utilizing sp^2 carbon-linked 3D COFs (JUC-580 and JUC-581) for sustained drug release and fluorescence imaging. The results demonstrated that JUC-581 not only serves as a promising material for drug delivery and sustained release but also excels as an excellent fluorescent dye for cellular imaging[129]. During the same year, the research team introduced a novel 3D COF named TUS-84. This structure featured a two-fold interpenetrating **scu-c** net, which was employed for the delivery and sustained release of ibuprofen. Impressively, about 12% of the ibuprofen was delivered within a 24-hour period. Extended and controlled drug release holds the potential to reduce dosing frequency and effectively manage long-term pain[130]. In the subsequent year, another research group presented TUS-64, a 3D COF based on a 4-connected porphyrin topology[131]. TUS-64 boasts an exceptionally low density and an extraordinarily large pore size within its 3D COF structure. These features make it a promising candidate for drug delivery and controlled release applications. Meanwhile, Wan *et al.* engineered a 3D COF with tetrathiafulvalene ligation designed for horseradish peroxidase. This sustained enzyme release process significantly prolongs the enzyme activity, particularly during enzyme prodrug therapy[132].

Separation of gas

Efficiently recovering H_2 from refinery waste gases containing H_2, CO_2, and CH_4 is a significant industrial goal in the pursuit of clean energy generation and the reduction of CO_2 emissions[104]. This endeavor aims to continually decrease CO_2 emissions, contributing to a cleaner environment. Additionally, the separation and capture of CO_2 from gas mixtures, such as flue gas, hold paramount importance in reducing carbon emissions[105]. In 2015, Lu *et al.* achieved a groundbreaking milestone by successfully cultivating 3D COF membranes on the surface of porous α-Al_2O_3, marking a breakthrough in using 3D COF for hydrogen and nitrogen methane separation. The resulting 3D COF-320 membrane exhibited an impressive hydrogen permeance of 5.67×10^{-7} $mol \cdot m^{-2} \cdot s \cdot Pa^{-1}$[65]. Fu *et al.* made notable contributions by fabricating COF-MOF composite membranes, enhancing the selectivity and separation of H_2/CO_2 gases. Notably, the separation factors for H_2/CO_2 mixtures were 12.6 and 13.5 for [COF-300]-[Zn_2(bdc)$_2$(dabco)] and [COF-300]-[ZIF-8] composite membranes, respectively[66]. Another pioneering achievement was the work of Guan *et al.*, who utilized ionic liquids at room temperature and pressure to synthesize a series of 3D-IL-COFs for CO_2/N_2 and CO_2/CH_4 separation[54]. These 3D COFs exhibited exceptionally high carbon dioxide capture rates at 298 K and 1 bar (5.34%, 7.61%, and 4.93%) due to strong ionic dipole interactions. They also observed high CO_2/N_2 separation (24.6, 24.0, and 24.4 for 3D-IL-COF-1, 3D-IL-COF-2, and 3D-IL-COF-3, respectively,) and CO_2/CH_4 adsorption selectivity (23.1 in 3D-IL-COF-1, 22.3 in 3D-IL-COF-2, and 21.5 in 3D-IL-COF-3).

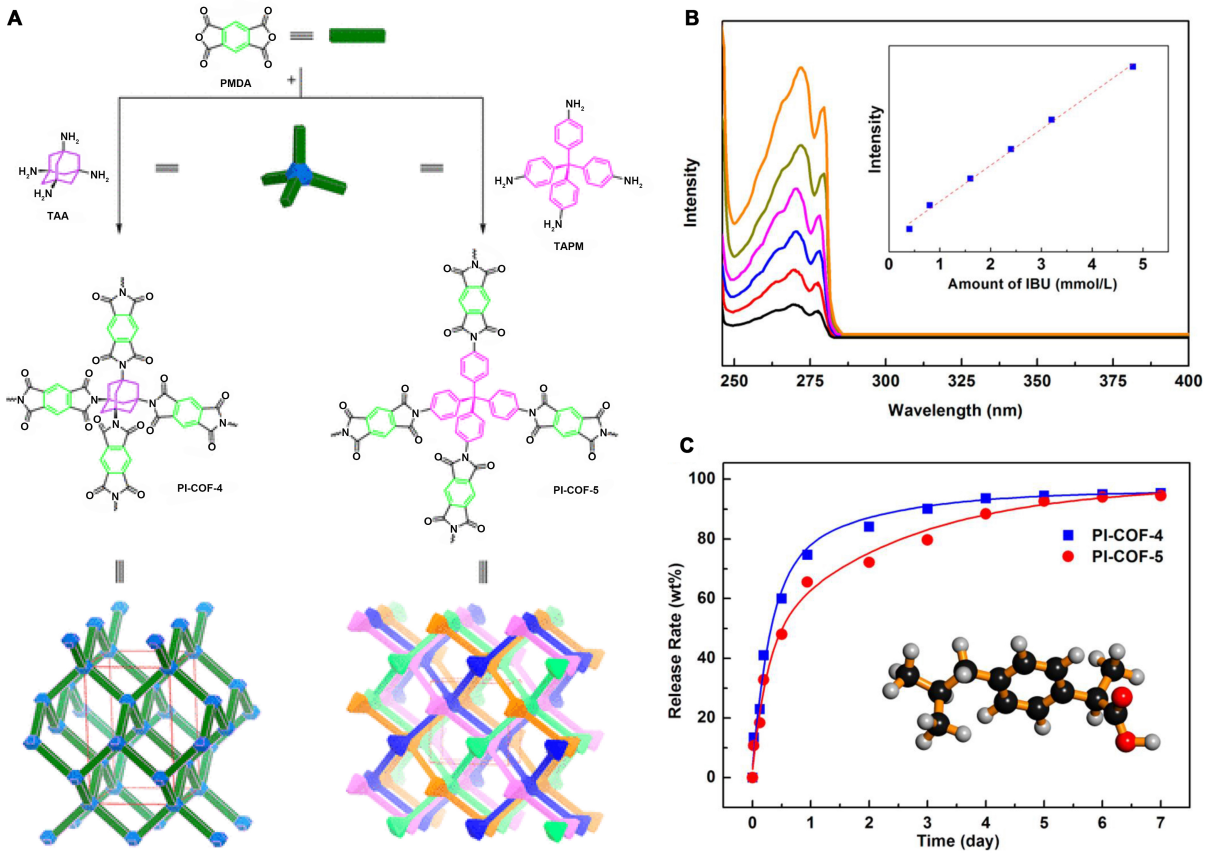

Figure 3. (A) Schematic diagram of the structures of PI-COFs for drug adsorption; (B) UV-vis spectra of ibuprofen in simulated body fluid at different concentrations; (C) Release profiles of ibuprofen -loaded 3D PI-COFs. Reproduced with permission from ref[48], Copyright 2015 from American Chemical Society. COFs: Covalent organic frameworks; 3D: three-dimensional.

Gao *et al.* reported three 3D-TPB-COFs with five-fold interpenetrated **pts** topology, which exhibited significantly higher CO_2 adsorption capacity than N_2 (approximately 90 $cm^3 \cdot g^{-1}$) at 273 K and 1 bar[80]. Cheng *et al.* ingeniously incorporated COF-300 into 6FDA-DAM and Pebax to create mixed matrix membranes for gas separation[133]. This innovation resulted in a 52% increase in CO_2 permeability for 6FDA-DAM and a 57% increase for Pebax, thereby enhancing gas separation efficiency. As demonstrated in Figure 4, Li *et al.* introduced a novel synthetic strategy for fabricating COF membranes, including 2D N-COF and 3D COF-300 membranes. Both membrane types exhibited outstanding selectivity for the mixture of H_2/CO_2 mixed gas, with a selectivity of 13.8 for the 2D COF membrane and 11 for the 3D COF membrane[134]. Ji *et al.* investigated three isostructural 3D-OC-COFs by introducing various substituted ligands through a novel *in situ* acid-base neutralization strategy for the first time[135]. Among the three COFs, 3D-OC-COF-OH demonstrated outstanding CO_2 capacity (89.2 $cm^3 \cdot g^{-1}$ at 273 K and 51.5 $cm^3 \cdot g^{-1}$ at 298 K) and relatively superior separation performance in CO_2/CH_4 or CO_2/N_2 mixed gas. Furthermore, Yang *et al.* introduced a novel 3D COF via imine condensation reaction using a symmetric corrole linker for the first time[136]. Notably, this COF exhibited higher selectivity for CO compared to N_2, O_2, and CO_2 compared to other porous materials. Fu *et al.* developed a dense and continuous 2,5-dimethoxyterephthalaldehyde (DMTA)-COF membrane containing ether oxygen functional groups. This membrane was covalently attached to a polyaniline-modified porous alumina substrate through *in situ* synthesis at room temperature and pressure. The H_2/CO_2 two-component separation factor was 8.3, corresponding to an H_2 permeation flux of 6.3×10^{-7} $mol \cdot m^{-2} \cdot s \cdot Pa^{-1}$[137]. Additionally, Yang *et al.* reported incorporating a 3D COF into 6FDA-DMA as a

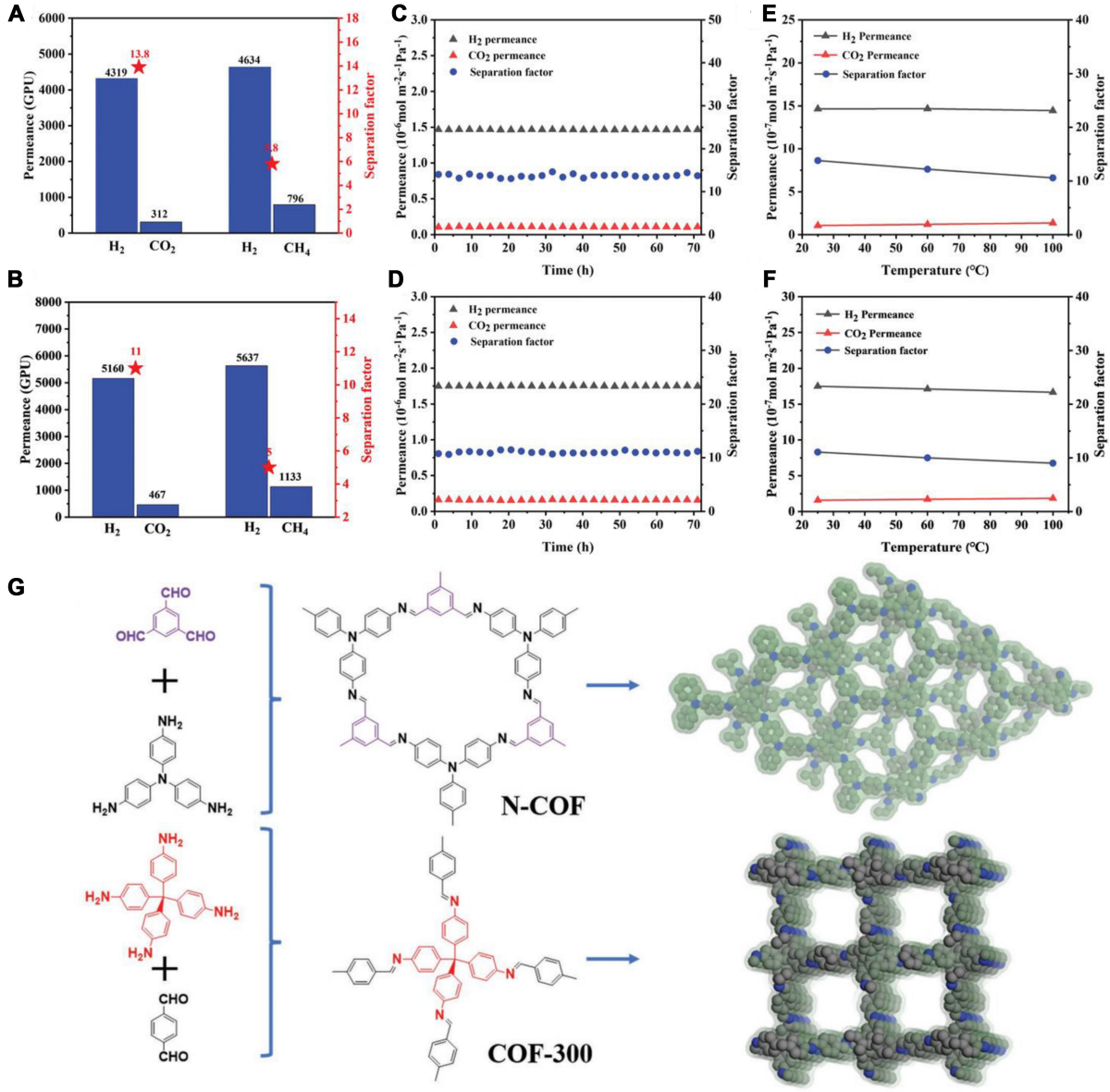

Figure 4. (A) Equimolar binary gas mixture separation performance of the N-COF Membrane; (B) Equimolar binary gas mixture separation performance of the COF-300 membrane; (C) Long-term test Results for the N-COF membrane using an equimolar H_2/CO_2 mixture at room temperature; (D) Long-term test results for the COF-300 membrane using an equimolar H_2/CO_2 mixture at room temperature; (E) Selectivity and permeance of the N-COF membrane as functions of temperature; (F) Selectivity and permeance of the COF-300 membrane as functions of temperature; (G) Schematic diagram of COF membrane structure for gas separation. Reproduced with Permission from ref[134], Copyright 2023, Wiley-VCH. COF: Covalent organic framework.

filler to form a mixed matrix membrane. This achieved a 57% increase in CO_2 permeability and an 18% increase in CO_2/CH_4 selectivity with a 10 wt% loading of the 3D-COF[138]. Gao *et al.* have reported a stimuli-responsive 3D-TPB-COF-HQ; the selectivity of CO_2/N_2 increases to a higher value of 93 after oxidation to 3D-TPB-COF-Q by using the ideal adsorbed solution theory[139]. The same group synthesized a series of alkyne-tagged 3D COFs, and azide is postmodified on the side chain via click reactions. The postmodified 3D-BMTA-COF-$[Ac]_{100\%}$ showed the mixture of CO_2/N_2 mixed gas selectivity of 78.9 at 273 K, which is about six times to non-modified 3D-BMTA-COF-$[C{\equiv}CH]_{100\%}$ [140]. Ethylene (C_2H_4), one of the most crucial chemical products in the petrochemical industry, is significant for separating ethylene from gases with

similar properties (CH_4, C_2H_6, C_2H_4, *etc.*)[141]. Baldwin *et al.* demonstrated that a highly porous 3D COF with Ni metalation DBA-3D-COF 1 exhibited ethane/ethylene selectivities of 1.25 and 1.28 at 0-0.1 bar at 273 K, and 1.24 and 1.15 at 295 K[142]. Jin *et al.* introduced an [8 + 2] approach to construct a series of 3D COFs with **bcu** net, with NKCOF-21 displaying excellent selectivity for ethylene, making it one of the best ethane-selective adsorbents for C_2H_4 purification (> 99.99%)[143]. Gong *et al.* prepared a pyrene-based 8-connected node 3D imine-linked COF with a 2-fold interpenetrated **bcu** topology, named ZJUT-3. This COF exhibited excellent selectivities of 48.2 for C_2H_2/CH_4 and 3.2 for C_2H_2/CO_2 at 1 bar[144].

Oil-water and dye separations

Water pollution, closely intertwined with human survival, has garnered increasing attention as a critical environmental issue[145]. The efficient removal of contaminants, such as oils and dyes, from water has become a focal point of research efforts[146]. Shi *et al.* have developed a 3D COF membrane with anti-swelling properties, utilizing interpenetrating imine bonds within its channels[147].

This membrane has exhibited remarkable stability, maintaining its performance for approximately 1,000 h when subjected to high-concentration feed. In another approach, Mohammed *et al.* utilized blocks containing halogen side chains to construct 3D-COF membranes with inherent hydrophobic characteristics. These membranes proved to be highly effective in demulsifying oil-water mixtures, achieving an impressive gravitational flux rate of 1,536 $L \cdot m^{-2} \cdot h^{-1}$[148]. Ma *et al.* engineered a hydrophobic 3D COF by introducing isopropyl groups into its structure. The 3D COF displayed exceptional stability, achieving separation efficiencies exceeding 99% and maintaining separation performance over at least 30 cycles when dealing with oil/water mixtures across a broad pH range[149].

Desalination and different ion separation

Desalination is of great significance for regions suffering from severe water scarcity[150]. Additionally, there are situations where it is essential to efficiently and selectively separate different ions from solutions[151]. Sun *et al.* constructed a 3D COF TAPM-Tp/nylon 6 membrane using a layer-by-layer approach, primarily for preliminary exploration of dye wastewater purification[152]. The TAPM-Tp/nylon 6 membrane exhibited negligible rejection rates for NaCl, Na_2SO_4, $MgCl_2$, and $MgSO_4$ (< 3.4%), while maintaining a high rejection rate for positively charged dyes. Shi *et al.* developed a 3D-COOH-COF Membrane designed for selective ion capture [Figure 5][153]. This membrane demonstrated exceptional selectivities, reaching up to 766 for K^+/Cu^{2+}, 634 for Na^+/Cu^{2+}, and 490 for Li^+/Cu^{2+}. The same research group reported a 3D-OH-COF grown *in situ* on cross-linked polyimide membranes in 2022, featuring sub-nanometer channels that efficiently screened monovalent and multivalent ions, achieving a K^+/Al^{3+} selectivity of > 800[154].

Chromatographic separation

Considering the high stability, insolubility in common solvents, and excellent adsorption selectivity of 3D COFs, these materials have the potential to become stationary phases in HPLC[155]. Han *et al.* synthesized the first 3D chiral COFs with a 4-fold interpenetrated structure through imine linkages[156]. Both chiral COFs (CCOF 5 and CCOF 6) can serve as stationary phases for HPLC, enabling efficient separation of racemic alcohols [Figure 6]. Porous materials containing metals have been shown to have some ability to separate aromatic hydrocarbon mixtures[157]. In 2019, Huang *et al.* developed a zinc (Zn)-coordinated 3D Salen COF as a stationary phase in an HPLC column for separating ethylbenzene and xylene isomers[68]. Qian *et al.* used a layer-by-layer assembly method to create COF- 300@SiO_2 composite as a stationary phase for HPLC. This phase efficiently and precisely separated isomers such as nitrophenol, nitroaniline, and aminophenol[158]. In 2022, the same group reported JNU-5, a 3D COF containing amino functional groups with a 9-fold-interpenetrated **dia** net, as a stationary phase for separating xylene isomers[159]. In the same year, they

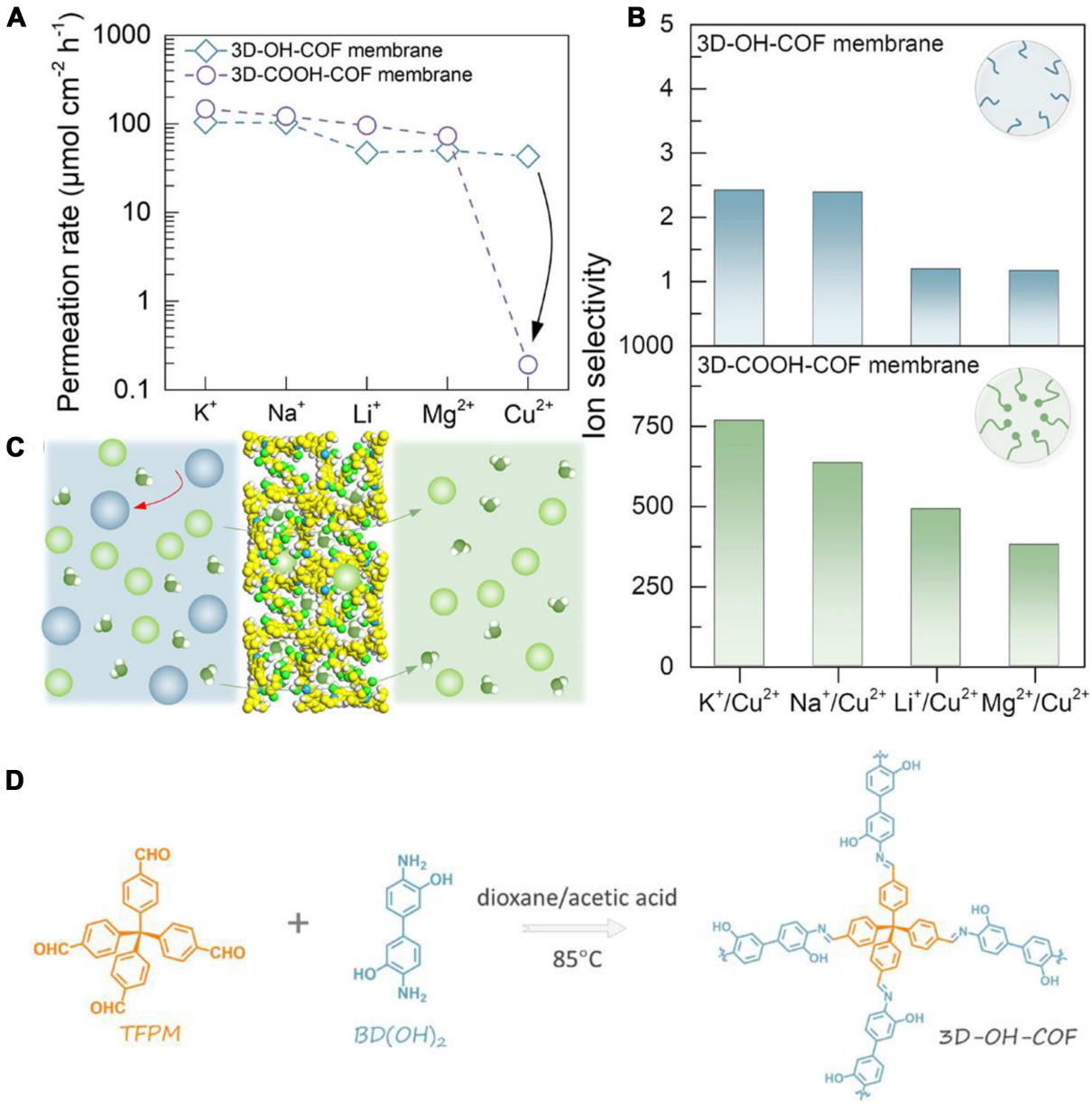

Figure 5. (A and B) Rates of ion permeation and the corresponding selectivity of the membranes; (C) Schematic diagram illustrating the selective ion capture by the 3D-COOH-COF; (D) Schematic diagram of 3D-OH-COF. Reproduced with permission from ref[153], Copyright 2021, American Chemical Society. 3D: Three-dimensional; COF: covalent organic framework.

introduced hydroxyl-functionalized 3D COF JNU-6 with a 5-fold interpenetrating diamond net for fast-selective solid-phase extraction of organophosphorus pesticides. This combination, along with gas chromatography-flame thermion detection, was used to detect four selected organophosphorus pesticides with detection limits as low as 3.0-15.0 ng·mL^{-1}[160]. Subsequently, the group reported an imine-based 3D COF with a four-fold interpenetrating **dia** net structure, prepared by a solvothermal method, as a stationary phase for HPLC. This COF efficiently separates acidic phenol mixtures and basic aniline mixtures[161]. In the following year, the same group reported single-crystal COF (SCOF-303) with different particle sizes, where a particle size of about 0.4 μm provided excellent separation of xylene isomers (with a resolution of 2.26-3.52 and efficiency of 7,879 plates·m^{-1})[162]. Zong *et al.* synthesized 3D TpTAM by ultrasound to evaluate its

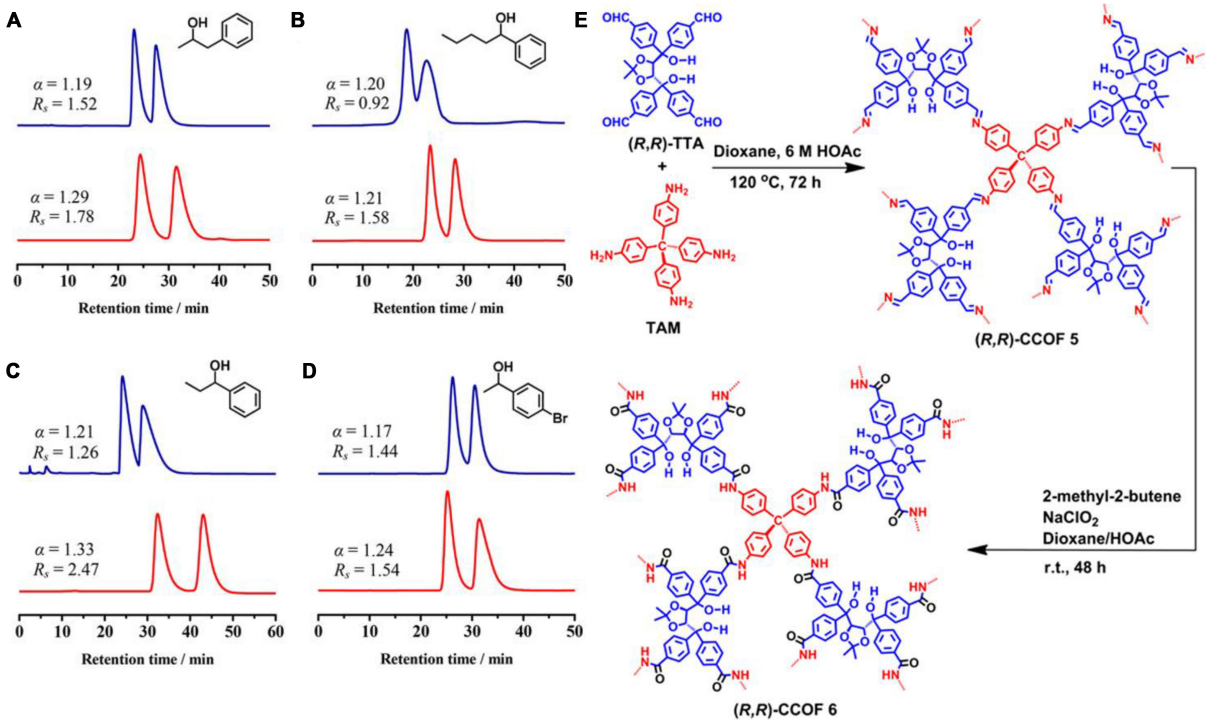

Figure 6. HPLC separation of (A) racemic 1-phenyl-2-propanol; (B) 1-phenyl-1-pentanol; (C) 1-phenyl-1-propanol; and (D) 1-(4-bromophenyl) ethanol on CCOF 5 (blue line) and CCOF 6 (red line) packed columns, respectively, using a hexane/isopropyl alcohol (v/v = 99:1) mobile phase at a flow rate of 0.2 mL/min; (E) Schematic diagram of preparing CCOF 5 and CCOF 6. Reproduced with permission from ref[156], Copyright 2019, American Chemical Society. HPLC: High-performance liquid chromatography.

potential as a stationary phase in capillary columns. They tested its performance in separating four fluoroquinolones[163]. In 2023, the same research group successfully synthesized JUC-515, introduced it into a capillary column, and thoroughly studied its effects on the isolation of fluoroquinolones, achieving excellent resolution (> 1.5)[164]. Niu *et al.* pioneered the *in-situ* growth of COF-300 on open-tubular capillary electrochromatography as a separation medium[165]. This medium efficiently separates organic compounds such as styrene, benzene, ethylbenzene, propylbenzene, naphthalene, methylbenzene, and 1-methylnaphthalene. Moroni *et al.* selected imine-linked 3D COFs, including COF-300 (COF-300-rt and COF-300-st), for the adsorption and separation of benzene and cyclohexane[120]. These COFs adsorb more benzene (251, 221, and 214 $cm^3 \cdot g^{-1}$ STP) than cyclohexane (175, 133, and 164 $cm^3 \cdot g^{-1}$ STP) at 298 K and 1 bar. Furthermore, COF-300 also demonstrated better separation efficiency for benzene and cyclohexane.

Heterogeneous catalysis

Thermal catalysis

Characterized by their abundant, continuous, and uniformly open channels, 3D COFs play a crucial role in facilitating mass transfer during catalysis. This feature positions them as a highly promising platform for catalytic applications[166]. Additionally, these 3D networks are insoluble and exceptionally stable, enabling easy separation from products or reactants and allowing for multiple recycling cycles[167]. Moreover, their continuous and uniform pores exhibit a certain degree of size selectivity. Through pre-modification or post-modification methods, active sites can be precisely anchored to the specific locations within these channels. This capability provides an ideal platform for conducting in-depth studies of catalytic mechanisms[168].

Thermal catalysis serves as a fundamental method for various organic reactions[169]. Fang *et al.* synthesized two innovative 3D imine-connected COFs, BF-COF-1 and BF-COF-2, and explored their application in the Knoevenagel condensation reaction[11]. BF-COF-1 exhibited excellent catalytic activity, achieving a high conversion rate of approximately 96%, while BF-COF-2 showed an even higher conversion rate of around 98%. Both BF-COFs displayed highly efficient size selectivity and recyclability, marking a pioneering use of 3D COFs as a catalytic platform. Meanwhile, 3D DL-COFs prepared by the same group underwent hydrolysis through acetal catalysis, facilitated by the acidic site of the boron oxide group, followed by Knoevenagel condensation catalyzed by the imine-bonded basic site[76]. Subsequently, the group developed two 3D radical-based COFs via a bottom-up approach (JUC-565 and JUC-566) containing radical moieties [Figure 7][170]. Notably, JUC-566 demonstrated remarkable catalytic universality for the aerobic oxidation of various alcohols to their corresponding aldehydes. In 2017, the team reported a copper-coordinated 3D COF with a salphen structure for catalytic elimination of superoxide radicals, exhibiting almost 100% catalytic efficiency[171]. More recently, they further engineered the triptycene-based 3D JUC-598 by confining FeS_x nanoparticles into its pore surface (JUC-598@FeS_x) for catalytic applications in Fenton reactions[172]. JUC-598@FeS_x exhibited excellent catalytic degradation efficiency for dyes, achieving 95% for crystalline violet and 91% for methylene blue within 90 min, respectively. Guan *et al.* synthesized a novel 3D azine-linked COF (3D-HNU5) with a 2-fold interpenetrated **dia** net, serving as an efficient catalyst for the cycloaddition of propargylic alcohols with CO_2 to produce carbonates[77]. Haque *et al.* designed and synthesized a zinc-coordinated 3D COF for catalyzing the formation of oxazolidinone and α-alkylene cyclic carbonate using carbon dioxide and propynol[173]. Liu *et al.* reported spirobifluorene (SP)-3D-COF- 2,2'-bipyridine (BPY), a 3D COF containing bipyridine building blocks, employing palladium and bipyridine coordination as catalyst for the Suzuki-Miyaura coupling reaction[174]. Additionally, the same group constructed tetraphenylmethane (TPM)-3D-COF-BPY, another 3D COF with bipyridine building blocks. In this case, Pd (II) selectively coordinated on the bipyridine coordination sites within the COF matrix and was subsequently reduced to palladium nanoparticles, serving as a catalyst for the Suzuki-Miyaura coupling reaction[175]. Hou *et al.* reported two 3D chiral COFs with interpenetrating open frames, acting as heterogeneous Brønsted acid catalysts for the asymmetric acetalation of aromatic aldehydes and 2-aminobenzamide, achieving impressive yields of 93%[176]. Huang *et al.* developed a 3D COF containing hydroxy groups for the reduction of 4-nitrophenol and the degradation of organic dyes after loading silver nanoparticles[177]. Jin *et al.* grew platinum nanoparticles *in-situ* within the pores of COF-300, enabling oxidase-like activity[178]. Ma *et al.* designed LZU-301, a 3D COF with a **dia** net structure containing pyridine functional groups within its pores, effectively catalyzing Knoevenagel condensation reactions and yielding a remarkable 72% yield after 6 h.[179]. Lastly, Gao *et al.* reported a composite of COF-300 and heteropoly acid (HPA) for the catalytic olefin epoxidation reaction[180].

Photocatalysis

In comparison to traditional thermal catalysis, photocatalytic technology requires only low-density solar energy and does not necessitate additional energy input during the process, rendering it an environmentally friendly green technology[181]. Meng *et al.* introduced the synthesis of two porphyrin-based materials, a 2D COF (2D-PdPor-COF) and a 3D COF (3D-PdPor-COF), and explored their applications as photocatalysts[182]. In contrast to 2D-PdPor-COF, 3D-PdPor-COF exhibited higher catalytic selectivity and efficiency in the catalytic reaction of sulfide oxidation to sulfoxide. Kumar *et al.* designed a 3D COF with a nine-fold interpenetrating **dia** net containing bipyridine functional groups[79]. This 3D COF can be employed as a photocatalyst for the oxidation of cyanide in an aqueous solution after chelation with ruthenium ions. Chao *et al.* developed a 3D non-interpenetrating **fjh** COF named 1,3,6,8-tetrakis-(aminophenyl)pyrene (TAPPy)- tris-formylphenylamine (TFPA) containing pyrene with mesoporous channels, displaying excellent catalytic activity for photo redox thiol-ene cross-coupling reactions and photoredox thiol radical-mediated acylation of amines into amides[183]. Jin *et al.* designed and synthesized

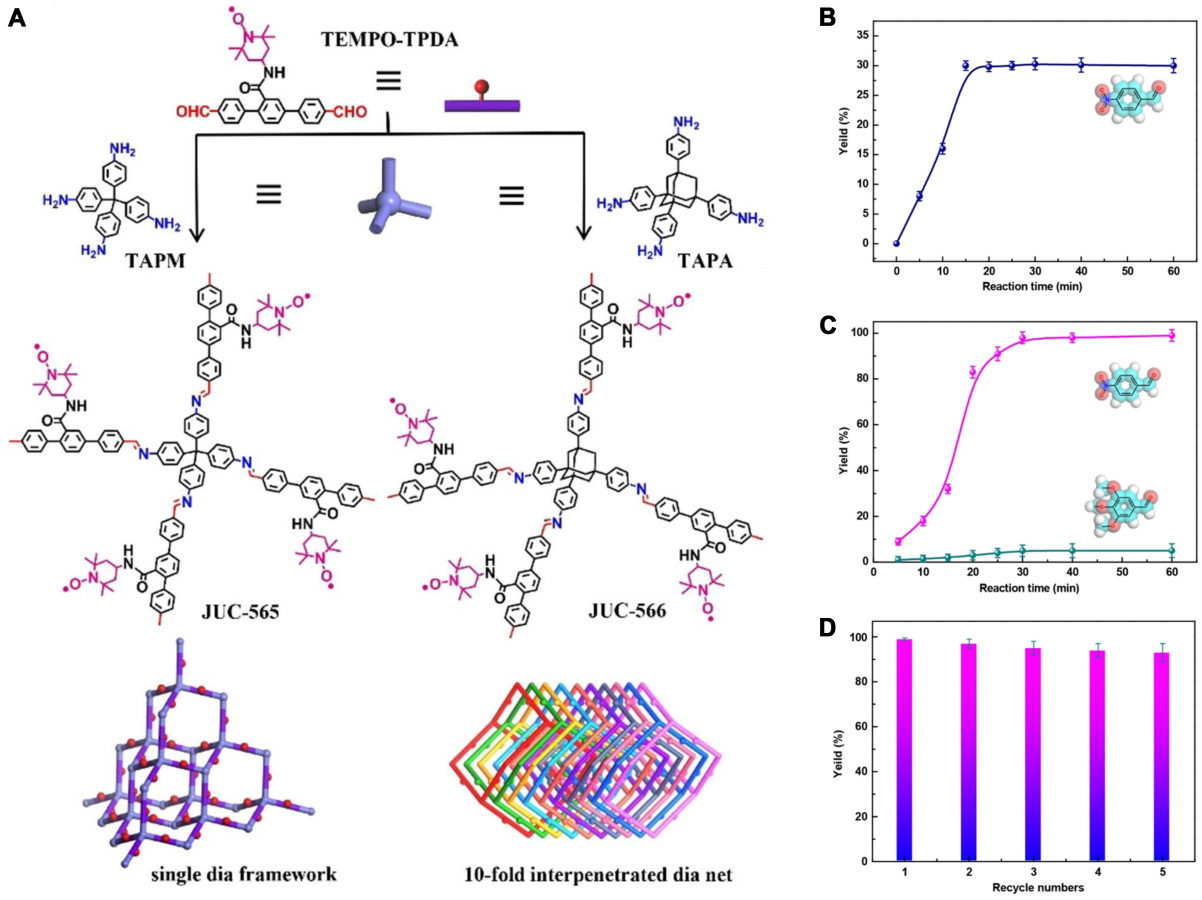

Figure 7. (A) Schematic diagram of preparing JUC-565 and JUC-566; (B) Yield *vs.* time curve for aerobic oxidation controlled by the addition or removal of COF crystals; (C) Yield *vs.* time curves for aerobic oxidation with substrates of different sizes; (D) Recyclability study of aerobic oxidation with 4-nitrobenzyl alcohol as the substrate. Reproduced with permission from ref[170], Copyright 2021 Wiley-VCH. COF: Covalent organic framework.

two highly crystalline 3D COFs (NKCOF-25-H and NKCOF-25-Ni) through an [8 + 4] approach with new **scu** topologies as photocatalysts for the cycloaddition of *tert*-aniline and maleimide under visible light[40]. Wang *et al.* prepared Fe_3O_4/COF-300 composites for effective photocatalysis in dye degradation in wastewater under 365 nm violet light irradiation[184]. Xu *et al.* constructed a new 3D COF named 5,10,15,20-tetra(4-aminophenyl)porphyrin (TAPP)-hexa(4-formylphenyl)benzene (HFPB)-COF) containing porphyrin units with a non-interpenetrated **she** net, providing active sites for the photocatalytic α-functionalization of aldehydes and CO_2 reduction reactions[23]. Yu *et al.* reported a 3D COF named N,N,N,N-tetrakis(4-aminophenyl)-1,4-benzenediamine and 5,5'-(2,1,3-benzothiadiazole-4,7-diyl) bis[2-thiophenecarboxaldehyde] (TPDT)-COF with a seven-fold interpenetrating structure[185]. Notably, the type of product obtained by photocatalysis (*cis*-stilbene or phenanthrene) can be altered by regulating the reaction gas environment, with a selectivity exceeding 99%. The same group also reported a series of 3D MCOFs based on covalent bonding between $Ru(bpy)_3^{2+}$/$Fe(bpy)_3^{2+}$ for efficient photocatalytic hydrogen production. Among them, Rubpy-ZnP achieved the highest H_2 generation rate (30,338 $\mu mol \cdot g^{-1} \cdot h^{-1}$), making it one of the most effective COF-based catalysts[186]. As shown in Figure 8, Ding *et al.* designed and synthesized a series of 3D COFs based on triptycene and porphyrin with an **stp** net, referred to as JUC-640-M, for photocatalysis[19]. Among them, JUC-640-Co was employed for photocatalytic CO_2 reduction and achieved an extremely high carbon monoxide yield (15.1 $mmol \cdot g^{-1} \cdot h^{-1}$) with ultra-high selectivity (94.4%).

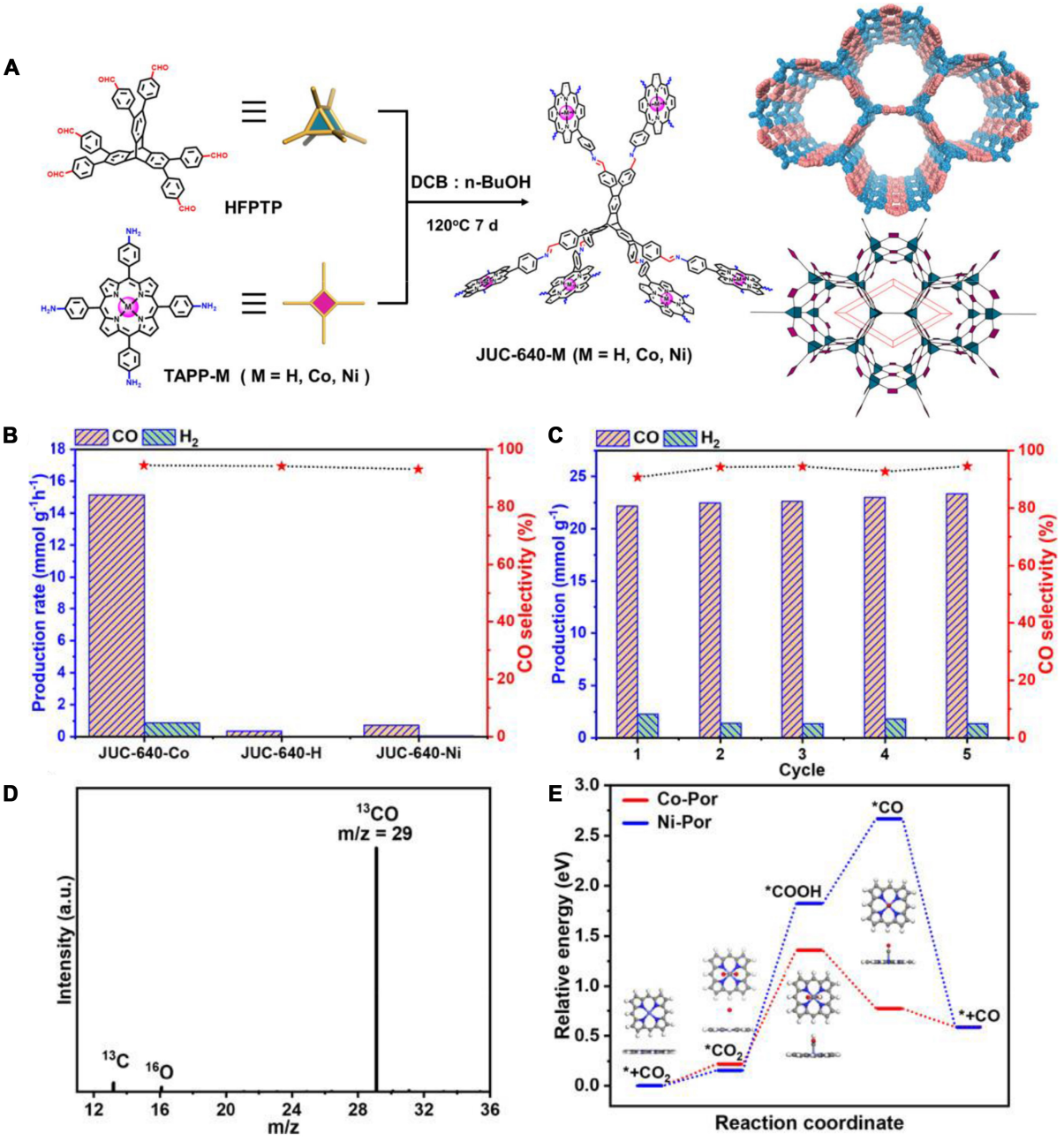

Figure 8. (A) Schematic diagram of preparing JUC-640-M; (B) Comparison of the photocatalytic activity of JUC-640-M under the following conditions: 3 mg of COF, 5 mg of $Ru(bpy)_3Cl_2·6H_2O$, 50 mg of BIH, 8 mL of MeCN, 12 mL of water, 300 W Xe lamp (≥ 380 nm), 1 h; (C) Durability measurements of JUC-640-Co (2 h per cycle); (D) ^{13}C isotopic experiment for JUC-640-Co; (E) Free energy diagrams for CO_2 reduction to CO on JUC-640-M (M = Co or Ni). Reproduced with permission from ref[19], Copyright 2023, American Chemical Society. COF: Covalent organic framework.

Dong *et al.* conducted similar research and developed π-conjugated 3D COFs (pNJU-318 and pNJU-319Fe) containing a hexabenzo-trinaphthalene structure for photocatalytic carbon dioxide reduction. Among them, pNJU-319Fe efficiently reduced carbon dioxide to carbon monoxide under visible light, with a yield of up to 68.8 μmol·g^{-1}·h^{-1}[187]. Wu *et al.* reported a 3D COF with a **tty** net, which displayed a high production rate (1,081 μmol·g^{-1}·h^{-1}) for the photocatalytic production of hydrogen peroxide[41]. Lin *et al.* reported two Cu-porphyrin-based 3D COFs as heterogeneous photocatalysts to produce singlet oxygen under

illumination[188]. Another porphyrin-linked 3D COF (COF-366) was designed and synthesized by Hynek *et al.*[189]. COF-366 can continuously produce singlet oxygen under visible light, inactivate bacteria, and achieve antibacterial effects. Zhang *et al.* constructed a porphyrin-based 3D COF with copper coordination named Cu@COF-1,3,5,7-Tetrakis(4-aminophenyl)adamantane and 5,10,15,20-tetrakis(4-benzaldehyde)porphyrin (TATB) in 2022 for use as a photocatalyst[190]. Cu@COF-TATB could produce singlet oxygen to induce immunogenic cell death (ICD) in cancer cells at 635 nm. Yan *et al.* reported a 3D fluorescent COF photocatalyst for the generation of singlet oxygen, which can control the capture and desorption of singlet oxygen to regulate the fluorescence intensity of the COF[191]. In 2021, Zhang *et al.* reported a series of ICD-active 3D COFs (COF-607, COF-608, and COF-609) to achieve the production of reactive oxygen species, resulting in excellent ICD induction efficacy[192]. Among them, COF-609 was tested in mice with breast cancer, and after 110 days of treatment, the mice had a survival rate of over 95%.

Electrocatalysis

In response to the rapid societal development, the human demand for energy is surging[193], but this heightened need, coupled with the excessive utilization of fossil fuels, has led to severe environmental pollution and an impending energy crisis[194]. Addressing these issues necessitates an improvement in energy efficiency and the exploration of cleaner energy sources[195]. In this context, electrochemical conversion processes have garnered significant attention due to their inherent advantages of high efficiency and minimal environmental impact[196]. These electrochemical processes encompass a range of reactions, including the oxygen reduction (ORR), oxygen evolution (OER), hydrogen evolution (HER), carbon dioxide reduction (CO_2RR), and nitrogen reduction reactions (NRR)[197], all of which rely on efficient catalysts to enable their efficient execution[198]. Liu *et al.* have undertaken the design and synthesis of two 3D COFs based on porphyrin, namely PCOF-1 and PCOF-2[199]. Notably, PCOF-1-Co exhibited an overpotential of 473 mV at a current density of 10 mA·cm^{-2}. Similarly, Gong *et al.* introduced a porphyrin-based 3D COF featuring a **stp** topology for electrocatalytic OER. Subsequent metallization with cobalt ions resulted in JUT-1@Co, which showcased a low overpotential of 295 mV at 10 mA·cm^{-2}[200]. Furthermore, Meng *et al.* developed a 3D porphyrin-based COF, which, after pyrolysis and coordination with iron and nickel ions, achieved a low overpotential of 328 mV at 10 mA·cm^{-2} in 0.1 M KOH for OER[201]. Tavakoli *et al.* designed a 3D COF incorporating porphyrin groups through an electropolymerization process, demonstrating an impressive electron transfer number of approximately 3.97 for ORR[202]. Additionally, Zhou *et al.* devised a catalyst composed of pyrolyzed COF-300-derived carbons loaded with platinum for the ORR, revealing a half-wave potential and onset potential of 0.85 and 0.98 V *vs.* reversible hydrogen electrode (RHE), respectively[203]. Li *et al.* achieved a significant milestone by introducing the first woven 3D COF, COF-112, as a catalyst[204]. Upon cobalt ion anchoring ($E_{1/2}$ = 0.76 V *vs.* RHE and n = 3.86), COF-112Co demonstrated exceptional ORR catalytic properties. Bao *et al.* successfully designed a fully conjugated 3D COF, Beijing University of Chemical Technology (BUCT)-COF-11, which, when combined with carbon nanotubes (CNTs), served as a high-efficiency, metal-free ORR electrocatalyst. The resulting BUCT-COF-11/CNT exhibited outstanding ORR activity, featuring a low half-wave potential of 0.72 V (*vs.* RHE)[205]. Chi *et al.* synthesized a 3D Co-porphyrin-based COF, for CO_2RR, achieving a remarkable CO faradaic efficiency of 92.4% at 0.6 V *vs.* RHE[206]. Lastly, Han *et al.* constructed 3D imide-bonded COFs with a **pts** network for CO_2RR, with CoPc-PI-COF-3 exhibiting a faradaic efficiency exceeding 88% for the conversion of CO_2 to CO, [Figure 9][207].

Carrier conduction and energy storage devices

Conductive

Due to its high degree of conjugation, 3D COF is regarded as a promising semiconductor material and exhibits excellent carrier mobility, making it a potential candidate for conducting materials[208]. Li *et al.* reported the first instance of a 3D conductive COF[209]. They doped I_2 into a TTF-based 3D COF to achieve a

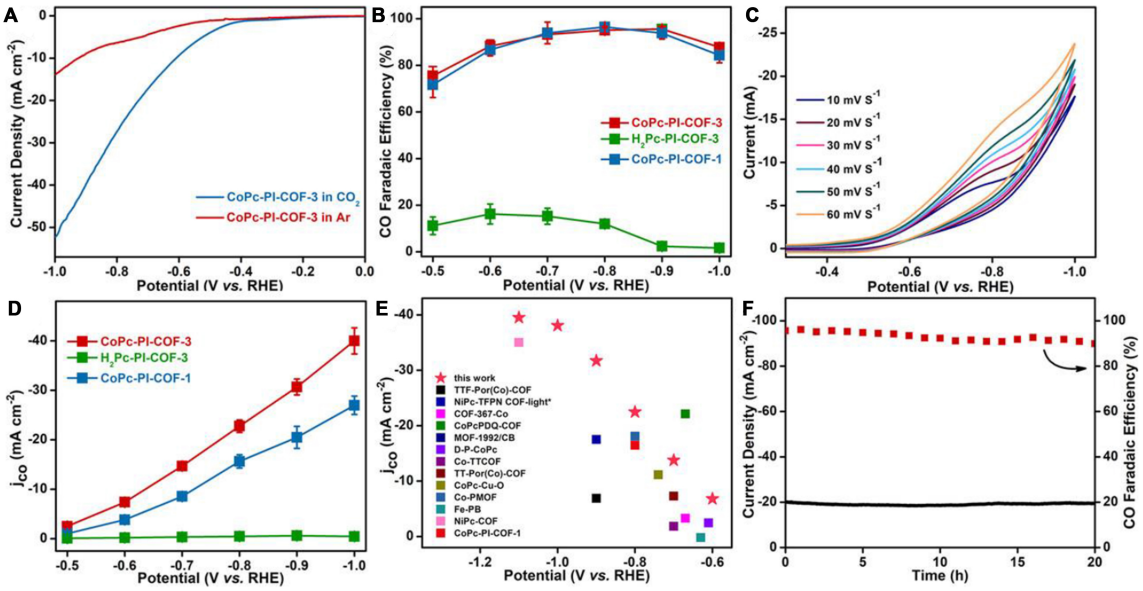
A
Current Density (mA cm-2)
Potential (V vs. RHE)
CoPc-PI-COF-3 in CO2
CoPc-PI-COF-3 in Ar
B
CO Faradaic Efficiency (%)
Potential (V vs. RHE)
CoPc-PI-COF-3
H2Pc-PI-COF-3
CoPc-PI-COF-1
C
Current (mA)
Potential (V vs. RHE)
10 mV S-1
20 mV S-1
30 mV S-1
40 mV S-1
50 mV S-1
60 mV S-1
D
jCO (mA cm-2)
Potential (V vs. RHE)
CoPc-PI-COF-3
H2Pc-PI-COF-3
CoPc-PI-COF-1
E
jCO (mA cm-2)
Potential (V vs. RHE)
this work
TTF-Por(Co)-COF
NiPc-TFPN COF-light*
COF-367-Co
CoPcPDQ-COF
MOF-1992/CB
D-P-CoPc
Co-TTCOF
TT-Por(Co)-COF
CoPc-Cu-O
Co-PMOF
Fe-PB
NiPc-COF
CoPc-PI-COF-1
F
Current Density (mA cm-2)
CO Faradaic Efficiency (%)
Time (h)

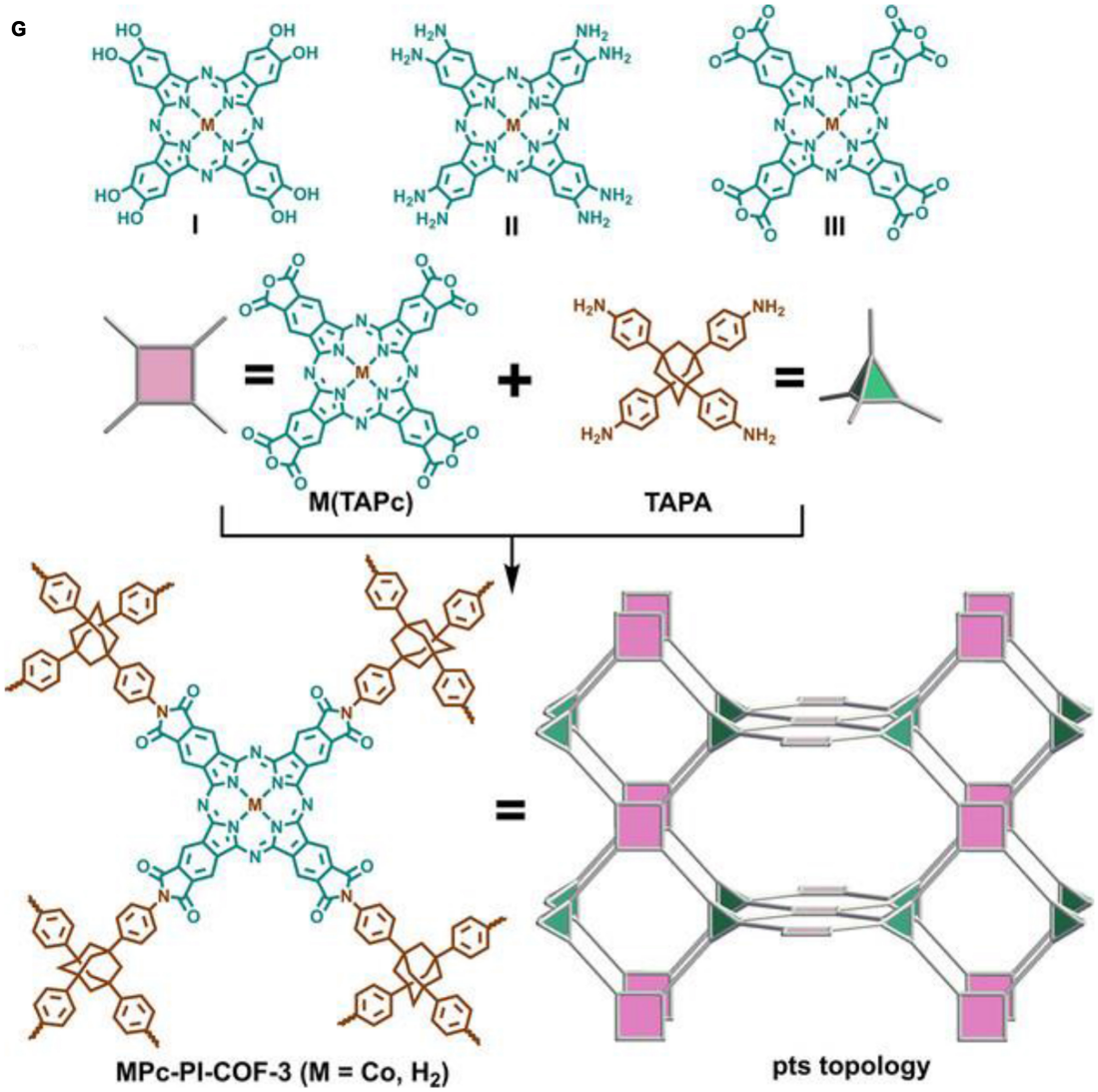
G
I
II
III
M(TAPc)
TAPA
MPc-PI-COF-3 (M = Co, H2)
pts topology

Figure 9. (A) LSV curves of CoPc-PI-COF-3 in CO_2 and Ar saturated electrolyte; (B) Faradaic efficiency diagrams of different COFs electrodes; (C) Scan rate dependence of cyclic voltammetry response of CoPc-PI-COF-3; (D) Partial CO current density of different COFs electrodes; (E) j_{CO} of 3D COF electrocatalyst and of Por/Pc-containing reticular materials performed in an H-type electrochemical cell; (F) Durability performance of 3D COF electrode at -0.80 V; (G) Schematic diagram of preparing MPc-PI-COF-3 with pts net. Reproduced with permission from ref[207], Copyright 2022, Wiley-VCH. COFs: Covalent organic frameworks; 3D: three-dimensional.

high conductivity of 1.4×10^{-2} S·cm^{-1} at 120 °C. The strategy of enhancing the conductivity of 3D COF through I_2 doping has also been successfully employed by Li *et al.*[210]. They used two different monomers with the same core to construct a 3D imine COF with **lvt** net, and the electrical conductivity reached as high as 1.5×10^{-4} S/cm. Wang *et al.* designed and synthesized a fully conjugated 3D COF termed BUCT-COF-1, which achieved an electron mobility of 2.75 cm^2·V^{-1}·s^{-1}[211]. The same research group also reported a sp^2 carbon-conjugated 3D COF (BUCT- COF-4) for the first time in the same year. It exhibited an electron mobility of 1.97 cm^2·V^{-1}·s^{-1} for the bare-COF and 2.62 cm^2·V^{-1}·s^{-1} after iodine doping[51]. Additionally, Yang *et al.* fabricated an all-carbon-linked 3D COF film, which exhibited a high electrical conductivity of 3.4 S·m^{-1} after doping with tetracyanoquinodimethane[212]. These advancements highlight the significant potential of 3D COFs as conducting materials in various applications.

Ion transport

Ion conductors play a crucial role in the electrolyte separators of energy storage devices, with lithium (Li)-ion and hydrogen-ion conduction being particularly significant in Li-ion batteries and fuel cells, attracting widespread attention[213]. Zhang *et al.* synthesized a 3D COF (CD-COF-Li) containing γ-cyclodextrin (γ-CD) for Li^+ transport. Impressively, it exhibited a high conductivity of up to 2.7 mS·cm^{-1} after doping with Li ions, making it one of the highest conductivities among crystalline organic porous materials at that time[42]. Furthermore, Wang *et al.* designed and synthesized a 3D COF with hydroxyl groups as a solid-state electrolyte. When combined with plastic crystals, these materials exhibited outstanding Li-ion conductivity (0.64 mS·cm^{-1}) and Li-ion transference numbers (0.7) at room temperature[214]. In the same year, Wu *et al.* reported three polyethylene glycol (PEG)-functionalized 3D COFs with different lengths of PEG chains. When combined with lithium bis((trifluoromethyl)sulfonyl)azanide (Li TFSI), these 3D COFs achieved an impressive ionic conductivity of 0.36 mS·cm^{-1} at 260 °C[215]. Moreover, Fan *et al.* fabricated a free-standing 3D COF membrane for H^+ ion transport, which achieved a remarkable conductivity of 0.650 S·cm^{-1} at 90 °C[216]. As shown in Figure 10, Yu *et al.* developed two 3D COFs functionalized with 12-crown-4 groups as an efficient nanofluidic platform for ion transport when combined with poly(ether sulfone)[217]. These COF-based mixed matrix membranes exhibited outstanding gating ratios, with values as high as 23.6, ranking among the best in metal ion-activated 1D nanochannels.

Energy storage devices

To date, 3D COFs have found successful applications in various energy storage devices, including Li batteries, Zn batteries, supercapacitors, and solar cells[218]. Yu *et al.* reported the use of 3D polyoxometalate COFs with a 3-fold interpenetrated **dia** net structure as anode materials for Li-ion batteries. These COFs exhibited a high reversible capacity exceeding 550 mA·h·g^{-1} and demonstrated impressive cycling stability, even after undergoing more than 500 cycles[219]. Schon *et al.* engineered a 3D framework based on perylene imide (PDI) for constructing a lithium battery cathode. This cathode achieved a high capacity of 75.9 mA·h·g^{-1} while maintaining near-100% coulomb efficiency and retaining over 80% of its capacity after 500 cycles[220]. In 2023, Chen *et al.* designed a fully π-conjugated 3D COF (PYTRI-COF-2) with an **ffc** net structure as anode materials for Li-ion batteries. This COF exhibited excellent cycling stability, with a capacity of 227.3 mA·h·g^{-1} after 450 cycles[221]. Wang *et al.* used CAGE-COF/S for Li-sulfur (S) batteries, achieving a capacity of up to 900 mAh·g^{-1} after 60 cycles[222]. Li *et al.* constructed a 3D COF called COF-301 with hydroxyl groups for Li-S batteries, known for its excellent long-term cycling stability (411.6 mA·h·g^{-1}

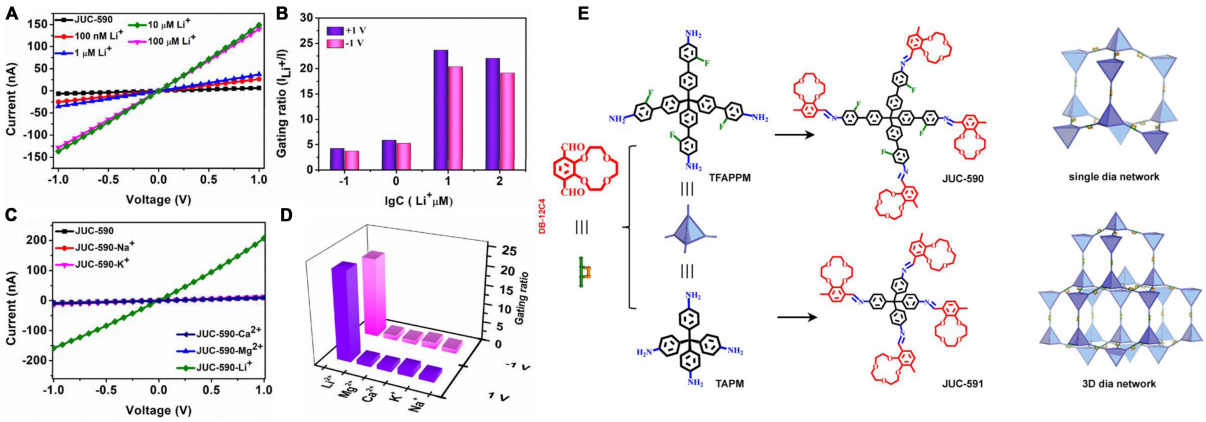

Figure 10. (A) The I-V curves of JUC-590-MMM before and after activation with different concentrations of Li^+; (B) The concentration-dependent changes in gating ratio (I_{Li}^+/I) of JUC-590-MMM at -1 and +1 V; (C) I-V curves of JUC-590-MMM after activation with different metal ions at -1 and +1 V; (D) The gating ratios of JUC-590-MMM after activation with different metal ions at -1 and +1 V; (E) Schematic diagram of preparing JUC-590 and JUC-591. Reproduced with permission from ref[217], Copyright 2022, Wiley-VCH.

after 500 cycles) at 0.5 C[223]. Liu *et al.* prepared two new 3D COFs with a homoaromatic conjugated structure and **scu** topology for Li-S batteries. They discovered that the high specific surface area and good charge transport improved the capacity (1,155 mA·h·g^{-1} at 0.2 C) and cycle stability (83% capacity retention at 2.0 C after 500 cycles) of the batteries[224]. As depicted in Figure 11, the same research group designed and synthesized a 3D COF containing 8-connected blocks for Li-S batteries in the second year, achieving a capacity of up to 1,249 mA·h·g^{-1} at 0.2 C and excellent stability (93% capacity retention at 0.5 C for 100 cycles), making it one of the best results reported so far for COF-based sulfur host materials for Li-S batteries[39]. Wu *et al.* reported a 3D COOH-functionalized COF film that was *in-situ* grown on bare zinc as a protective layer. This COF film significantly enhanced the long-term cycling stability of Zn batteries, maintaining a coulomb efficiency of more than 99.5% after 2,000 h[225]. Wu *et al.* constructed two SP-based 3D COFs (SP-3D-COF 1 and SP-3D-COF 2) for solar cells. These COFs improved the power conversion efficiency by 15.9% (SP-3D-COF 1) and 18.0% (SP-3D-COF 2)[226]. Biradar *et al.* created a 3D COF called tris(4-formylphenyl) phosphate (PFM)-COF1 for supercapacitors, which exhibited a capacitance of 158 F·g^{-1} at 0.5 A·g^{-1} and a power density of 1,077.72 W·kg^{-1}[227]. Chen *et al.* designed a strategy to encapsulate charged dye into the pores of 3D COFs for harvesting salinity gradient energy, resulting in a power density of 51.4 W·m^{-2} by mixing seawater and river water[228].

Fluorescence and sensors

Fluorescence sensing

Fluorescent COFs enhance the fluorescence properties of COF materials by incorporating chromophores such as triazine, pyrene, s-tetrazine, and triphenylene[229]. These fluorescent COFs can be utilized as sensors to detect persistent organic pollutants and analytes, including metal ions, organic explosives, fullerene derivatives, or biomolecules that significantly affect the fluorescence intensity of substances[230]. Lin *et al.* pioneered the design and synthesis of the first fluorescent pyrene-based 3D COF (3D-Py-COF) for explosive detection[29]. This fluorescent COF enabled sensitive detection of picric acids, exhibiting a quenching degree of 20% at a picric acid concentration of 75 ppm. The same research group also introduced a fluorescent 3D COF [3D-tetraphenylethylene (TPE)-COF] with a cluster-induced luminescent agent building block in 2018[231]. Notably, 3D-TPE-COF emits yellow fluorescence upon excitation, with a quantum yield of approximately 20%. Coating it on a commercial blue light-emitting diode can convert it into a white light-emitting diode with no significant intensity attenuation for 1,200 h. In 2023, the same group reported another 3D fluorescent COF designed for the detection of trace antibiotics in water. This

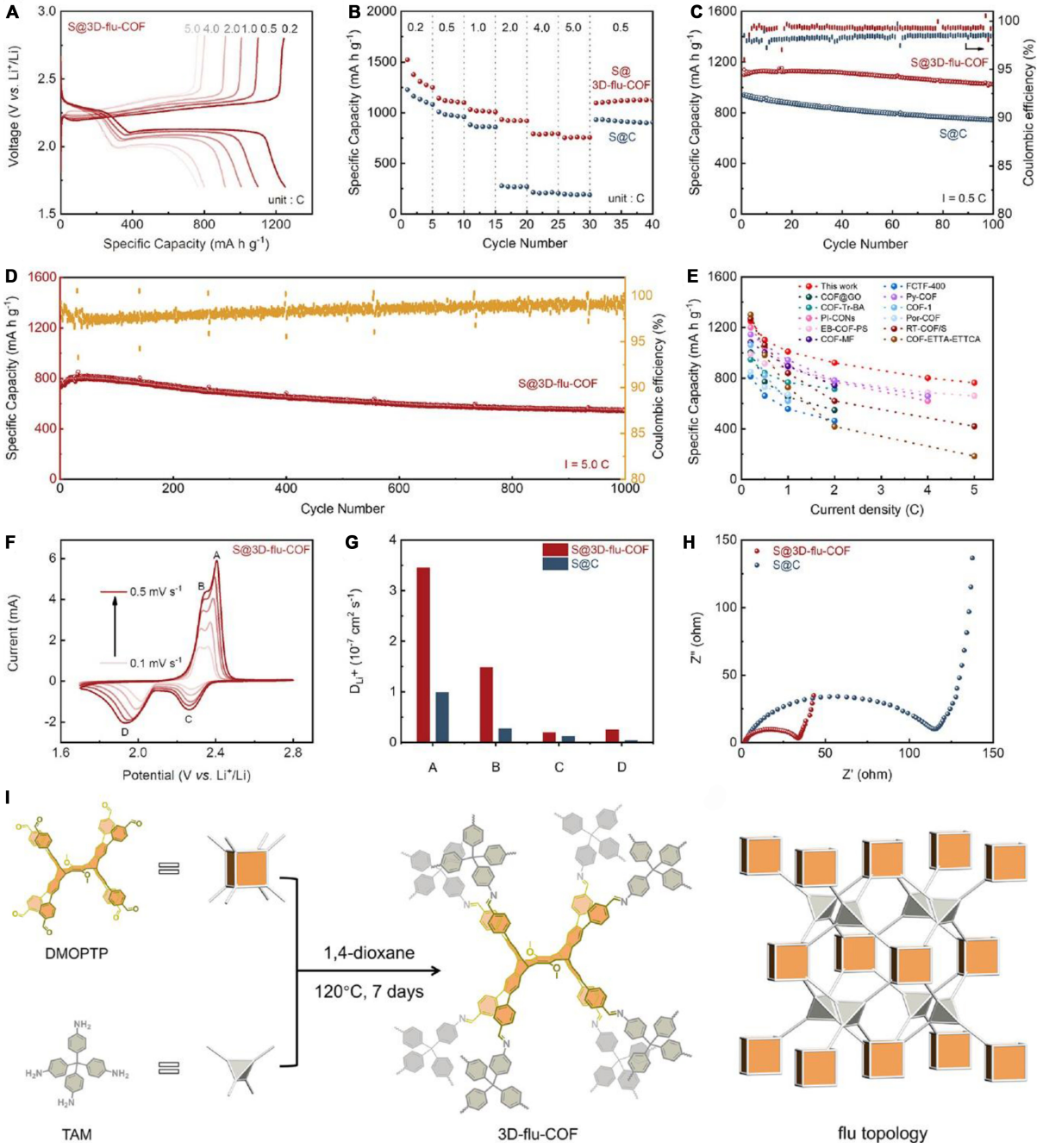

Figure 11. (A) Galvanostatic charge/discharge profiles of the S@3D-flu-COF electrode at various rates; (B) Rate performance of the S@3D-flu-COF and S@C electrodes at various rates; (C) Cycling stability of the S@3D-flu-COF and S@C electrodes at 0.5 C; (D) Cycling stability of the S@3D-flu-COF electrode at 5.0 C; (E) Comparison of the rate performances of COF-based sulfur host materials; (F) CVs of the S@3D-flu-COF electrode at scan rates ranging from 0.1 to 0.5 $mV \cdot s^{-1}$; (G) Li^+ diffusion coefficient of S@3D-flu-COF and S@C electrodes; (H) Nyquist plots of the S@3D-flu-COF and S@C electrodes; (I) Schematic diagram of preparing 3D-flu-COF with flu net. Reproduced with permission from ref[39], Copyright 2022, American Chemical Society. 3D: Three-dimensional; COF: covalent organic framework.

COF gradually quenches as the amount of nitrofurazone (a typical antibiotic) increases, with a maximum quenching efficiency of up to 93%[232]. Yuan *et al.* developed a 3D porous aromatic frameworks (PAF) named PAF-15 with an absolute quantum yield of fluorescence of up to 14% in methylene chloride, applied

for the molecular detection of explosives[233]. Li *et al.* created a COOH-functionalized 3D-COF used for adsorption and fluorescence detection of 9,10-phenanthraquinone after europium ions coordinated with it[234]. In 2021, Wu *et al.* prepared two fully conjugated 3D COFs from a saddle-like molecule containing thiophene as a tetrahedral node[235]. This research revealed that the prepared fluorescent COFs exhibit selective sensitivity to picric acids. Wang *et al.* reported a bipyridine-based 3D COF for fluorescence sensing of Co^{2+}. This COF serves as a fluorescent probe, displaying low detection limits and good recovery in cobalt ion detection[236]. Wei *et al.* constructed a 3D fluorescent COF (dynaCOF) with an acceptor-donor-acceptor (A-D-A) π coupling system for the detection of various organic vapors. This fluorescence sensor offers high sensitivity and low detection limits and maintains satisfactory stability and moisture resistance[237]. Chi *et al.* prepared COF-300 loaded with gold nanoparticles, followed by $CsPbBr_3$ quantum dots, as a fluorescence sensor for the determination of benzo(a)pyrene in cooking oil[238].

Other sensors and optics

Zhao *et al.* pioneered the design and synthesis of two 3D COFs completed with hydrazone motifs as pH-triggered molecular switches. They explored applications of these COFs in stimulus-responsive drug delivery systems[239]. At a pH of 4.8, the release of Ara-C increases nearly three-fold compared to a pH of 7.4. This enhancement holds significant promise for improving drug targeting and minimizing side effects. The same research group also created two dynamic 3D COFs, named JUC-635 and JUC-636, based on aggregation-induced emission or aggregation-induced quenching chromophores. As depicted in Figure 12, these COFs were employed for the first time to investigate pressure-induced color changes using diamond anvil pool technology[240]. Notably, JUC-635 maintains its fluorescence even under high pressure up to 3 GPa and exhibits reversible piezochromism at 12 GPa. This achievement marks high-contrast compression piezochromism with significant emission differences of up to 187 nm, making it one of the highest-performing piezochromism-based crystalline porous materials reported to date. Liu *et al.* engineered a flexible 3D COF named flexible COF (FCOF)-5 containing C–O bonds with a 6-fold interpenetrated **pts** net[241]. When mixed with polyvinylidene fluoride, the resulting film can reversibly absorb tetrahydrofuran vapor, triggering shape changes. Dong *et al.* utilized the interface method to synthesize a 3D self-supporting COF film at the air-water interface. This film also exhibits irreversible electrochromic behavior and can be used for anti-counterfeiting labels[242]. Similar applications have also been reported by Yan *et al.*, who designed a 3D fluorescent COF to control changes in COF fluorescence intensity by manipulating the COF's capture or release of singlet oxygen[191]. Furthermore, Bourda *et al.* prepared a bipyridine(bidy)-based 3D COF (Bipy COF) that exhibited a certain level of fluorescence intensity and excellent temperature sensing performance after coordination with lanthanides[243]. Peng *et al.* developed a method for the rapid synthesis of single-crystal 3D COFs using supercritical fluids. This approach displayed extraordinary potential in the fields of polarized photonics and nonlinear optics[64].

CONCLUSION AND OUTLOOK

Since El-Kaderi *et al.* first reported 3D COFs in 2007, these materials have received considerable attention from researchers due to their high specific surface area, adjustable pore size, and interpenetrating pore structures[2]. Currently, 3D COFs have found successful applications in various fields, including for adsorption, separation, heterogeneous catalysis, electrochemistry, energy storages, and sensors. The structure-activity relationship is paramount for the practical application of COFs. Researchers consistently strive to finely control their performance through optimal structural design. COF materials exhibit excellent crystallinity and stability, allowing the construction of an ideal periodic structure using different building block elements. This characteristic positions COFs as an ideal carrier material for establishing a structure-activity relationship. Consequently, crystallinity becomes a prerequisite for COFs to transition into industrial application production.

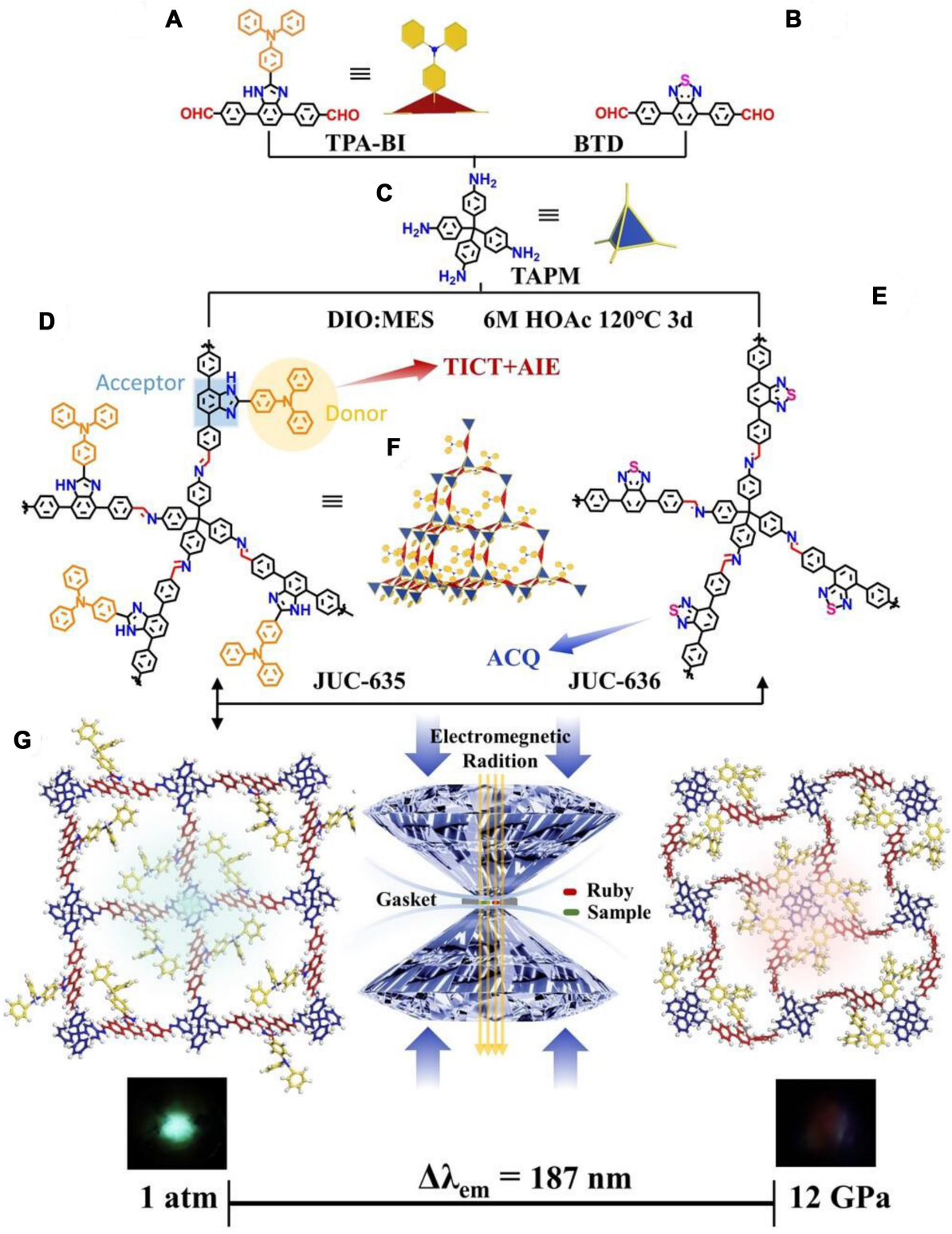

Figure 12. (A-C) constitute the monomers of JUC-635 and JUC-636; (D and E) Schematic diagram of JUC-635 and JUC-636. and JUC-636; (F) The two COFs have 10-fold interpenetrated dia net; (G) These materials were further used to study the pressure change behavior, demonstrating structural transformations in response to mechanical stimulation by DAC techniques. Reproduced with permission from ref[240], Copyright 2023, Wiley-VCH. COFs: Covalent organic frameworks.

The synthesis of highly crystalline COF frameworks typically involves reversible covalent bonds, which, while offering some advantages, also comes with limitations. These bonds are prone to decomposition under extreme conditions, significantly restricting their application scenarios. Conversely, the use of irreversible covalent bonds can yield highly stable COF materials, but often at the expense of poor crystallinity, hindering their ability to achieve high performance. Additionally, the strict deoxidation operation required for COF material synthesis imposes constraints on macro-preparation and large-scale applications. As a result, the synthesis strategy and efficient preparation of highly stable and crystalline COF materials pose a major challenge in the practical application of this field. Addressing this issue will become another significant obstacle in the development of COFs, especially for 3D COFs.

When compared to 2D COFs, 3D COFs still exhibit certain limitations. Firstly, due to the limited diversity of building blocks available for constructing 3D COFs, the number of reported 3D COFs remains relatively low, at less than 200, which hampers the exploration of their full potential in various applications. Secondly, the synthesis methods for 3D COFs are comparatively restricted, and they lack the strong π-π stacking interactions that are prevalent in 2D COFs, making it more challenging to achieve highly crystalline materials. Stability is also a significant challenge for 3D COFs. Hence, designing highly stable 3D COFs, by means with stable linkage, shall explore more. On the other hand, while the interpenetrating pore structure can enhance stability to some extent, it may lead to reduced exposure of functional groups within the pores and low specific surface area. Finally, the current applications of 3D COFs primarily revolve around adsorption, separation, sensing, catalysis, and energy storage, but many of these studies are relatively superficial. Further research into machine and system regulation is needed, requiring more attention from researchers. Moreover, expanding the application of 3D COFs into broader fields is essential. In summary, we have outlined the research progress of 3D COFs in their existing applications. This article emphasizes the potential applications for functional 3D COFs, encompassing separation, adsorption, heterogeneous catalysis, energy storage, and sensing. We believe that this review can offer valuable guidance for the synthesis and functionalization of functional 3D COFs in the future.

DECLARATIONS

Authors' contributions

Responsible for the overall design, direction and supervision of the project: Fang Q
Performed the writing of the manuscript: Wang R
Discussed the results and contributed to the writing of the manuscript: Zhao J, Qiu S

Availability of data and materials

Not applicable.

Financial support and sponsorship

This work was supported by National Key R&D Program of China (2021YFF0500504 and 2022YFB3704900), National Natural Science Foundation of China (22025504, 21621001, and 22105082), the SINOPEC Research Institute of Petroleum Processing, "111" project (BP0719036 and B17020), and the program for JLU Science and Technology Innovative Research Team.

Conflicts of interest

All authors declared that there are no conflicts of interest.

Ethical approval and consent to participate

Not applicable.

Consent for publication

Not applicable.

REFERENCES

1. Guan X, Chen F, Fang Q, Qiu S. Design and applications of three dimensional covalent organic frameworks. *Chem Soc Rev* 2020;49:1357-84. DOI
2. El-Kaderi HM, Hunt JR, Mendoza-Cortés JL, et al. Designed synthesis of 3D covalent organic frameworks. *Science* 2007;316:268-72. DOI
3. Guan X, Fang Q, Yan Y, Qiu S. Functional regulation and stability engineering of three-dimensional covalent organic frameworks. *Acc Chem Res* 2022;55:1912-27. DOI PubMed
4. Fang Q, Ma S. Covalent organic frameworks. *Macromol Rapid Commun* 2023;44:e2300203. DOI PubMed
5. Guan X, Chen F, Qiu S, Fang Q. Three-dimensional covalent organic frameworks: from synthesis to applications. *Angew Chem Int Ed Engl* 2023;62:e202213203. DOI PubMed
6. Yusran Y, Guan X, Li H, Fang Q, Qiu S. Postsynthetic functionalization of covalent organic frameworks. *Natl Sci Rev* 2020;7:170-90. DOI PubMed PMC
7. Yusran Y, Fang Q, Qiu S. Postsynthetic covalent modification in covalent organic frameworks. *Isr J Chem* 2018;58:971-84. DOI
8. Nguyen HL. Reticular design and crystal structure determination of covalent organic frameworks. *Chem Sci* 2021;12:8632-47. DOI PubMed PMC
9. Gropp C, Canossa S, Wuttke S, et al. Standard practices of reticular chemistry. *ACS Cent Sci* 2020;6:1255-73. DOI PubMed PMC
10. Lyu H, Ji Z, Wuttke S, Yaghi OM. Digital reticular chemistry. *Chem* 2020;6:2219-41. DOI
11. Fang Q, Gu S, Zheng J, Zhuang Z, Qiu S, Yan Y. 3D microporous base-functionalized covalent organic frameworks for size-selective catalysis. *Angew Chem Int Ed Engl* 2014;53:2878-82. DOI
12. Evans AM, Ryder MR, Ji W, et al. Trends in the thermal stability of two-dimensional covalent organic frameworks. *Faraday Discuss* 2021;225:226-40. DOI
13. Ma X, Scott TF. Approaches and challenges in the synthesis of three-dimensional covalent-organic frameworks. *Commun Chem* 2018;1:98. DOI
14. Tran QN, Lee HJ, Tran N. Covalent organic frameworks: from structures to applications. *Polymers* 2023;15:1279. DOI PubMed PMC
15. Vardhan H, Nafady A, Al-Enizi AM, Ma S. Pore surface engineering of covalent organic frameworks: structural diversity and applications. *Nanoscale* 2019;11:21679-708. DOI
16. Ma T, Li J, Niu J, et al. Observation of interpenetration isomerism in covalent organic frameworks. *J Am Chem Soc* 2018;140:6763-6. DOI
17. Garai B, Shetty D, Skorjanc T, et al. Taming the topology of calix[4]arene-based 2D-covalent organic frameworks: interpenetrated vs noninterpenetrated frameworks and their selective removal of cationic dyes. *J Am Chem Soc* 2021;143:3407-15. DOI
18. Li Y, Chen W, Xing G, Jiang D, Chen L. New synthetic strategies toward covalent organic frameworks. *Chem Soc Rev* 2020;49:2852-68. DOI
19. Ding J, Guan X, Lv J, et al. Three-dimensional covalent organic frameworks with ultra-large pores for highly efficient photocatalysis. *J Am Chem Soc* 2023;145:3248-54. DOI
20. Chang J, Chen F, Li H, et al. Three-dimensional covalent organic frameworks with nia nets for efficient separation of benzene/cyclohexane mixtures. *Nat Commun* 2024;15:813. DOI PubMed PMC
21. Yahiaoui O, Fitch AN, Hoffmann F, Fröba M, Thomas A, Roeser J. 3D anionic silicate covalent organic framework with srs topology. *J Am Chem Soc* 2018;140:5330-3. DOI PubMed
22. Nguyen HL, Gropp C, Ma Y, Zhu C, Yaghi OM. 3D covalent organic frameworks selectively crystallized through conformational design. *J Am Chem Soc* 2020;142:20335-9. DOI
23. Xu X, Cai P, Chen H, Zhou HC, Huang N. Three-dimensional covalent organic frameworks with she topology. *J Am Chem Soc* 2022;144:18511-7. DOI
24. Lan Y, Han X, Tong M, et al. Materials genomics methods for high-throughput construction of COFs and targeted synthesis. *Nat Commun* 2018;9:5274. DOI PubMed PMC
25. Kang X, Han X, Yuan C, Cheng C, Liu Y, Cui Y. Reticular synthesis of tbo topology covalent organic frameworks. *J Am Chem Soc* 2020;142:16346-56. DOI
26. Zhu D, Zhu Y, Chen Y, et al. Three-dimensional covalent organic frameworks with pto and mhq-z topologies based on Tri- and tetratopic linkers. *Nat Commun* 2023;14:2865. DOI PubMed PMC
27. Wang X, Bahri M, Fu Z, et al. A cubic 3D covalent organic framework with nbo topology. *J Am Chem Soc* 2021;143:15011-6. DOI
28. Uribe-Romo FJ, Hunt JR, Furukawa H, Klöck C, O'Keeffe M, Yaghi OM. A crystalline imine-linked 3-D porous covalent organic

framework. *J Am Chem Soc* 2009;131:4570-1. DOI PubMed
29. Lin G, Ding H, Yuan D, Wang B, Wang C. A pyrene-based, fluorescent three-dimensional covalent organic framework. *J Am Chem Soc* 2016;138:3302-5. DOI
30. Liu Y, Li J, Lv J, et al. Topological isomerism in three-dimensional covalent organic frameworks. *J Am Chem Soc* 2023;145:9679-85. DOI
31. Ma T, Kapustin EA, Yin SX, et al. Single-crystal x-ray diffraction structures of covalent organic frameworks. *Science* 2018;361:48-52. DOI
32. Xie Y, Li J, Lin C, et al. Tuning the topology of three-dimensional covalent organic frameworks via steric control: from pts to unprecedented ljh. *J Am Chem Soc* 2021;143:7279-84. DOI
33. Li H, Ding J, Guan X, et al. Three-dimensional large-pore covalent organic framework with stp topology. *J Am Chem Soc* 2020;142:13334-8. DOI
34. Li H, Chen F, Guan X, et al. Three-dimensional triptycene-based covalent organic frameworks with ceq or acs topology. *J Am Chem Soc* 2021;143:2654-9. DOI PubMed
35. Li Z, Sheng L, Wang H, et al. Three-dimensional covalent organic framework with ceq topology. *J Am Chem Soc* 2021;143:92-6. DOI
36. Yu C, Li H, Wang Y, et al. Three-dimensional triptycene-functionalized covalent organic frameworks with hea net for hydrogen adsorption. *Angew Chem Int Ed Engl* 2022;61:e202117101. DOI
37. Gropp C, Ma T, Hanikel N, Yaghi OM. Design of higher valency in covalent organic frameworks. *Science* 2020;370:eabd6406. DOI PubMed
38. Shan Z, Wu M, Zhu D, et al. 3D covalent organic frameworks with interpenetrated pcb topology based on 8-connected cubic nodes. *J Am Chem Soc* 2022;144:5728-33. DOI
39. Liu W, Wang K, Zhan X, et al. Highly connected three-dimensional covalent organic framework with flu topology for high-performance Li-S batteries. *J Am Chem Soc* 2023;145:8141-9. DOI
40. Jin F, Lin E, Wang T, et al. Rationally fabricating 3D porphyrinic covalent organic frameworks with scu topology as highly efficient photocatalysts. *Chem* 2022;8:3064-80. DOI
41. Wu M, Shan Z, Wang J, Liu T, Zhang G. Three-dimensional covalent organic framework with tty topology for enhanced photocatalytic hydrogen peroxide production. *Chem Eng J* 2023;454:140121. DOI
42. Zhang Y, Duan J, Ma D, et al. Three-dimensional anionic cyclodextrin-based covalent organic frameworks. *Angew Chem Int Ed Engl* 2017;56:16313-7. DOI
43. Martínez-Abadía M, Strutyński K, Lerma-Berlanga B, et al. π-interpenetrated 3D covalent organic frameworks from distorted polycyclic aromatic hydrocarbons. *Angew Chem Int Ed Engl* 2021;60:9941-6. DOI
44. Lu HS, Han WK, Yan X, Chen CJ, Niu T, Gu ZG. A 3D anionic metal covalent organic framework with soc topology built from an octahedral Ti(IV) complex for photocatalytic reactions. *Angew Chem Int Ed Engl* 2021;60:17881-6. DOI PubMed
45. Lyle SJ, Waller PJ, Yaghi OM. Covalent organic frameworks: organic chemistry extended into two and three dimensions. *Trends Chem* 2019;1:172-84. DOI
46. Hunt JR, Doonan CJ, LeVangie JD, Côté AP, Yaghi OM. Reticular synthesis of covalent organic borosilicate frameworks. *J Am Chem Soc* 2008;130:11872-3. DOI PubMed
47. Stewart D, Antypov D, Dyer MS, et al. Stable and ordered amide frameworks synthesised under reversible conditions which facilitate error checking. *Nat Commun* 2017;8:1102. DOI PubMed PMC
48. Fang Q, Wang J, Gu S, et al. 3D porous crystalline polyimide covalent organic frameworks for drug delivery. *J Am Chem Soc* 2015;137:8352-5. DOI
49. Sun R, Wang X, Wang X, Tan B. Three-dimensional crystalline covalent triazine frameworks via a polycondensation approach. *Angew Chem Int Ed Engl* 2022;61:e202117668. DOI
50. Beaudoin D, Maris T, Wuest JD. Constructing monocrystalline covalent organic networks by polymerization. *Nat Chem* 2013;5:830-4. DOI PubMed
51. Wang S, Li XX, Da L, et al. A three-dimensional sp^2 carbon-conjugated covalent organic framework. *J Am Chem Soc* 2021;143:15562-6. DOI
52. Zhu Y, Long H, Zhang W. Imine-linked porous polymer frameworks with high small gas (H_2, CO_2, CH_4, C_2H_2) uptake and CO_2/N_2 selectivity. *Chem Mater* 2013;25:1630-5. DOI
53. Hu J, Huang Z, Liu Y. Beyond solvothermal: alternative synthetic methods for covalent organic frameworks. *Angew Chem Int Ed Engl* 2023;62:e202306999. DOI PubMed
54. Guan X, Ma Y, Li H, et al. Fast, ambient temperature and pressure ionothermal synthesis of three-dimensional covalent organic frameworks. *J Am Chem Soc* 2018;140:4494-8. DOI
55. Kappe CO. Controlled microwave heating in modern organic synthesis. *Angew Chem Int Ed Engl* 2004;43:6250-84. DOI PubMed
56. Estel L, Poux M, Benamara N, Polaert I. Continuous flow-microwave reactor: where are we? *Chem Eng Process* 2017;113:56-64. DOI
57. Campbell NL, Clowes R, Ritchie LK, Cooper AI. Rapid microwave synthesis and purification of porous covalent organic frameworks. *Chem Mater* 2009;21:204-6. DOI
58. Khan NA, Jhung SH. Synthesis of metal-organic frameworks (MOFs) with microwave or ultrasound: rapid reaction, phase-

selectivity, and size reduction. *Coord Chem Rev* 2015;285:11-23. DOI

59. Gogate PR, Sutkar VS, Pandit AB. Sonochemical reactors: important design and scale up considerations with a special emphasis on heterogeneous systems. *Chem Eng J* 2011;166:1066-82. DOI
60. Zhao W, Yan P, Yang H, et al. Using sound to synthesize covalent organic frameworks in water. *Nat Synth* 2022;1:87-95. DOI
61. He J, Jiang X, Xu F, et al. Low power, low temperature and atmospheric pressure plasma-induced polymerization: facile synthesis and crystal regulation of covalent organic frameworks. *Angew Chem Int Ed Engl* 2021;60:9984-9. DOI
62. Zhang YB, Su J, Furukawa H, et al. Single-crystal structure of a covalent organic framework. *J Am Chem Soc* 2013;135:16336-9. DOI
63. Evans AM, Castano I, Brumberg A, et al. Emissive single-crystalline boroxine-linked colloidal covalent organic frameworks. *J Am Chem Soc* 2019;141:19728-35. DOI
64. Peng L, Sun J, Huang J, et al. Ultra-fast synthesis of single-crystalline three-dimensional covalent organic frameworks and their applications in polarized optics. *Chem Mater* 2022;34:2886-95. DOI
65. Lu H, Wang C, Chen J, et al. A novel 3D covalent organic framework membrane grown on a porous α-Al_2O_3 substrate under solvothermal conditions. *Chem Commun* 2015;51:15562-5. DOI
66. Fu J, Das S, Xing G, Ben T, Valtchev V, Qiu S. Fabrication of COF-MOF composite membranes and their highly selective separation of H_2/CO_2. *J Am Chem Soc* 2016;138:7673-80. DOI PubMed
67. Yang Y, Chen Y, Izquierdo-Ruiz F, Schäfer C, Rahm M, Börjesson K. A self-standing three-dimensional covalent organic framework film. *Nat Commun* 2023;14:220. DOI PubMed PMC
68. Huang J, Han X, Yang S, et al. Microporous 3D covalent organic frameworks for liquid chromatographic separation of xylene isomers and ethylbenzene. *J Am Chem Soc* 2019;141:8996-9003. DOI
69. Bunck DN, Dichtel WR. Internal functionalization of three-dimensional covalent organic frameworks. *Angew Chem Int Ed Engl* 2012;51:1885-9. DOI PubMed
70. Xu L, Zhou X, Tian WQ, et al. Surface-confined single-layer covalent organic framework on single-layer graphene grown on copper foil. *Angew Chem Int Ed Engl* 2014;53:9564-8. DOI
71. Tao R, Ma X, Wei X, Jin Y, Qiu L, Zhang W. Porous organic polymer material supported palladium nanoparticles. *J Mater Chem A* 2020;8:17360-91. DOI
72. Zeng Y, Zou R, Zhao Y. Covalent organic frameworks for CO_2 Capture. *Adv Mater* 2016;28:2855-73. DOI PubMed
73. Guo X, Qiao Z, Liu D, Zhong C. Mixed-matrix membranes for CO_2 separation: role of the third component. *J Mater Chem A* 2019;7:24738-59. DOI
74. Furukawa H, Yaghi OM. Storage of hydrogen, methane, and carbon dioxide in highly porous covalent organic frameworks for clean energy applications. *J Am Chem Soc* 2009;131:8875-83. DOI PubMed
75. Li H, Pan Q, Ma Y, et al. Three-dimensional covalent organic frameworks with dual linkages for bifunctional cascade catalysis. *J Am Chem Soc* 2016;138:14783-8. DOI
76. Li Z, Li H, Guan X, et al. Three-dimensional ionic covalent organic frameworks for rapid, reversible, and selective ion exchange. *J Am Chem Soc* 2017;139:17771-4. DOI
77. Guan P, Qiu J, Zhao Y, et al. A novel crystalline azine-linked three-dimensional covalent organic framework for CO_2 capture and conversion. *Chem Commun* 2019;55:12459-62. DOI
78. Zhu Q, Wang X, Clowes R, et al. 3D cage COFs: a dynamic three-dimensional covalent organic framework with high-connectivity organic cage nodes. *J Am Chem Soc* 2020;142:16842-8. DOI PubMed PMC
79. Kumar G, Singh M, Goswami R, Neogi S. Structural dynamism-actuated reversible CO_2 adsorption switch and postmetalation-induced visible light C_α-H photocyanation with rare size selectivity in N-functionalized 3D covalent organic framework. *ACS Appl Mater Interfaces* 2020;12:48642-53. DOI
80. Gao C, Li J, Yin S, et al. Isostructural three-dimensional covalent organic frameworks. *Angew Chem Int Ed Engl* 2019;58:9770-5. DOI
81. Zhang L, Wang D, Cong M, et al. Construction of rigid amine-linked three-dimensional covalent organic frameworks for selectively capturing carbon dioxide. *Chem Commun* 2023;59:4911-4. DOI
82. Song J, Wang Z, Liu Y, et al. A three-dimensional covalent organic framework for CO_2 uptake and dyes adsorption. *Chem Res Chin Univ* 2022;38:834-7. DOI
83. Reardon H, Hanlon JM, Hughes RW, Godula-jopek A, Mandal TK, Gregory DH. Emerging concepts in solid-state hydrogen storage: the role of nanomaterials design. *Energy Environ Sci* 2012;5:5951-79. DOI
84. Zhu L, Zhang YB. Crystallization of covalent organic frameworks for gas storage applications. *Molecules* 2017;22:1149. DOI PubMed PMC
85. Chen Z, Kirlikovali KO, Idrees KB, Wasson MC, Farha OK. Porous materials for hydrogen storage. *Chem* 2022;8:693-716. DOI
86. Nemiwal M, Sharma V, Kumar D. Improved designs of multifunctional covalent-organic frameworks: hydrogen storage, methane storage, and water harvesting. *MROC* 2021;18:1026-36. DOI
87. Kalidindi SB, Oh H, Hirscher M, et al. Metal@COFs: covalent organic frameworks as templates for Pd nanoparticles and hydrogen storage properties of Pd@COF-102 hybrid material. *Chem* 2012;18:10848-56. DOI
88. Li Z, Sheng L, Hsueh C, et al. Three-dimensional covalent organic frameworks with hea topology. *Chem Mater* 2021;33:9618-23. DOI

89. Liao L, Guan X, Zheng H, et al. Three-dimensional microporous and mesoporous covalent organic frameworks based on cubic building units. *Chem Sci* 2022;13:9305-9. DOI PubMed PMC
90. Alahakoon SB, Thompson CM, Occhialini G, Smaldone RA. Design principles for covalent organic frameworks in energy storage applications. *ChemSusChem* 2017;10:2116-29. DOI PubMed
91. Chang F, Zhou J, Chen P, et al. Microporous and mesoporous materials for gas storage and separation: a review. *Asia Pacific J Chem Eng* 2013;8:618-26. DOI
92. Feng X, Ding X, Jiang D. Covalent organic frameworks. *Chem Soc Rev* 2012;41:6010-22. DOI PubMed
93. Ma H, Ren H, Meng S, et al. A 3D microporous covalent organic framework with exceedingly high C_3H_8/CH_4 and C_2 hydrocarbon/CH_4 selectivity. *Chem Commun* 2013;49:9773-5. DOI
94. Kurisingal JF, Yun H, Hong CS. Porous organic materials for iodine adsorption. *J Hazard Mater* 2023;458:131835. DOI PubMed
95. Skorjanc T, Shetty D, Trabolsi A. Pollutant removal with organic macrocycle-based covalent organic polymers and frameworks. *Chem* 2021;7:882-918. DOI
96. Yang Y, Tu C, Yin H, Liu J, Cheng F, Luo F. Molecular iodine capture by covalent organic frameworks. *Molecules* 2022;27:9045. DOI PubMed PMC
97. Wang C, Wang Y, Ge R, et al. A 3D covalent organic framework with exceptionally high iodine capture capability. *Chem* 2018;24:585-9. DOI
98. Wang G, Xie K, Zhu F, et al. Construction of tetrathiafulvalene-based covalent organic frameworks for superior iodine capture. *Chem Res Chin Univ* 2022;38:409-14. DOI
99. Chang J, Li H, Zhao J, et al. Tetrathiafulvalene-based covalent organic frameworks for ultrahigh iodine capture. *Chem Sci* 2021;12:8452-7. DOI PubMed PMC
100. Liu T, Zhao Y, Song M, et al. Ordered macro-microporous single crystals of covalent organic frameworks with efficient sorption of iodine. *J Am Chem Soc* 2023;145:2544-52. DOI
101. Zou J, Wen D, Zhao Y. Flexible three-dimensional diacetylene functionalized covalent organic frameworks for efficient iodine capture. *Dalton Trans* 2023;52:731-6. DOI
102. Wu C, Xia L, Xia S, Van der Bruggen B, Zhao Y. Advanced covalent organic framework-based membranes for recovery of ionic resources. *Small* 2023;19:2206041. DOI
103. Yu J, Yuan L, Wang S, et al. Phosphonate-decorated covalent organic frameworks for actinide extraction: a breakthrough under highly acidic conditions. *CCS Chem* 2019;1:286-95. DOI
104. Cao S, Li B, Zhu R, Pang H. Design and synthesis of covalent organic frameworks towards energy and environment fields. *Chem Eng J* 2019;355:602-23. DOI
105. Huang L, Liu R, Yang J, et al. Nanoarchitectured porous organic polymers and their environmental applications for removal of toxic metal ions. *Chem Eng J* 2021;408:127991. DOI
106. Zhang CR, Cui WR, Xu RH, et al. Alkynyl-based sp^2 carbon-conjugated covalent organic frameworks with enhanced uranium extraction from seawater by photoinduced multiple effects. *CCS Chem* 2021;3:168-79. DOI
107. Cui W, Chen Y, Xu W, et al. A three-dimensional luminescent covalent organic framework for rapid, selective, and reversible uranium detection and extraction. *Sep Purif Technol* 2023;306:122726. DOI
108. Zhang C, Qi J, Cui W, et al. A novel 3D sp^2 carbon-linked covalent organic framework as a platform for efficient electro-extraction of uranium. *Sci China Chem* 2023;66:562-9. DOI
109. Chen Y, Wang X, Xu W, et al. Constructing redox-active 3D covalent organic frameworks with high-affinity hexameric binding sites for enhanced uranium capture. *Chem Eng J* 2023;459:141633. DOI
110. Liu Y, Pang H, Wang X, et al. Zeolitic imidazolate framework-based nanomaterials for the capture of heavy metal ions and radionuclides: a review. *Chem Eng J* 2021;406:127139. DOI
111. Liu M, Kong H, Bi S, et al. Non-interpenetrated 3D covalent organic framework with dia topology for Au ions capture. *Adv Funct Mater* 2023;33:2302637. DOI
112. Nandanwar SU, Coldsnow K, Utgikar V, Sabharwall P, Eric Aston D. Capture of harmful radioactive contaminants from off-gas stream using porous solid sorbents for clean environment - a review. *Chem Eng J* 2016;306:369-81. DOI
113. Zhang CR, Cui WR, Yi SM, et al. An ionic vinylene-linked three-dimensional covalent organic framework for selective and efficient trapping of ReO_4^- or $^{99}TcO_4^-$. *Nat Commun* 2022;13:7621. DOI PubMed PMC
114. Wang Y, Lan J, Yang X, et al. Superhydrophobic phosphonium modified robust 3D covalent organic framework for preferential trapping of charge dispersed oxoanionic pollutants. *Adv Funct Mater* 2022;32:2205222. DOI
115. Li B, Chen J, Xiao J, Zhao L, Qiu H. Nanoporous sulfonic covalent organic frameworks for selective adsorption and separation of lanthanide elements. *ACS Appl Nano Mater* 2023;6:2498-506. DOI
116. Lu Q, Ma Y, Li H, et al. Postsynthetic functionalization of three-dimensional covalent organic frameworks for selective extraction of lanthanide ions. *Angew Chem Int Ed Engl* 2018;57:6042-8. DOI
117. Wang L, Liu J, Wang J, Huang J. Bifunctional thiophene-based covalent organic frameworks for Hg^{2+} removal and I_2 vapor adsorption. *Chem Eng J* 2023;473:145405. DOI
118. Zhang Y, Li H, Chang J, et al. 3D thioether-based covalent organic frameworks for selective and efficient mercury removal. *Small* 2021;17:2006112. DOI
119. Gendy EA, Oyekunle DT, Ifthikar J, Jawad A, Chen Z. A review on the adsorption mechanism of different organic contaminants by

covalent organic framework (COF) from the aquatic environment. *Environ Sci Pollut Res Int* 2022;29:32566-93. DOI

120. Moroni M, Roldan-Molina E, Vismara R, Galli S, Navarro JAR. Impact of pore flexibility in imine-linked covalent organic frameworks on benzene and cyclohexane adsorption. *ACS Appl Mater Interfaces* 2022;14:40890-901. DOI PubMed PMC
121. Li Z, Hsueh C, Tang Z, et al. Rational design of imine-linked three-dimensional mesoporous covalent organic frameworks with bor topology. *SusMat* 2022;2:197-205. DOI
122. Mohammed AK, Ali JK, Kuzhimully MBS, et al. The fragmented 3D-covalent organic framework in cellulose acetate membrane for efficient phenol removal. *Chem Eng J* 2023;466:143234. DOI
123. Lu F, Lin J, Lin C, Qi G, Lin X, Xie Z. Heteroporous 3D covalent organic framework-based magnetic nanospheres for sensitive detection of bisphenol A. *Talanta* 2021;231:122343. DOI
124. Lu F, Wu M, Lin C, Lin X, Xie Z. Efficient and selective solid-phase microextraction of polychlorinated biphenyls by using a three-dimensional covalent organic framework as functional coating. *J Chromatogr A* 2022;1681:463419. DOI
125. Li W, Xue Y, Fu X, Ma Z, Feng J. Covalent organic framework reinforced hollow fiber for solid-phase microextraction and determination of pesticides in foods. *Food Control* 2022;133:108587. DOI
126. Walker G, Weatherley L. Adsorption of dyes from aqueous solution - the effect of adsorbent pore size distribution and dye aggregation. *Chem Eng J* 2001;83:201-6. DOI
127. Liu Y, Ma Y, Yang J, et al. Molecular weaving of covalent organic frameworks for adaptive guest inclusion. *J Am Chem Soc* 2018;140:16015-9. DOI
128. Esrafili A, Wagner A, Inamdar S, Acharya AP. Covalent organic frameworks for biomedical applications. *Adv Healthc Mater* 2021;10:e2002090. DOI PubMed
129. Liao L, Zhang Z, Guan X, et al. Three-dimensional sp^2 carbon-linked covalent organic frameworks as a drug carrier combined with fluorescence imaging. *Chin J Chem* 2022;40:2081-8. DOI
130. Das S, Sekine T, Mabuchi H, et al. Three-dimensional covalent organic framework with scu-c topology for drug delivery. *ACS Appl Mater Interfaces* 2022;14:48045-51. DOI PubMed PMC
131. Zhao Y, Das S, Sekine T, et al. Record ultralarge-pores, low density three-dimensional covalent organic framework for controlled drug delivery. *Angew Chem Int Ed Engl* 2023;62:e202300172. DOI
132. Wan X, Yin J, Yan Q, et al. Sustained-release nanocapsule based on a 3D COF for long-term enzyme prodrug therapy of cancer. *Chem Commun* 2022;58:5877-80. DOI
133. Cheng Y, Zhai L, Ying Y, et al. Highly efficient CO_2 capture by mixed matrix membranes containing three-dimensional covalent organic framework fillers. *J Mater Chem A* 2019;7:4549-60. DOI
134. Li B, Wang Z, Gao Z, et al. Self-standing covalent organic framework membranes for H_2/CO_2 separation. *Adv Funct Mater* 2023;33:2300219. DOI
135. Ji C, Su K, Wang W, et al. Tunable cage-based three-dimensional covalent organic frameworks. *CCS Chem* 2022;4:3095-105. DOI
136. Yang J, André L, Desbois N, Gros C, Brandès S. 2D/3D covalent organic frameworks based on cobalt corroles for CO binding. *Mater Today Chem* 2023;28:101357. DOI
137. Fu J, Ben T. Fabrication of a novel covalent organic framework membrane and its gas separation performance. *Acta Chim Sinica* 2020;78:805-14. DOI
138. Yang Y, Goh K, Weerachanchai P, Bae T. 3D covalent organic framework for morphologically induced high-performance membranes with strong resistance toward physical aging. *J Membrane Sci* 2019;574:235-42. DOI
139. Gao C, Li J, Yin S, Sun J, Wang C. Redox-triggered switching in three-dimensional covalent organic frameworks. *Nat Commun* 2020;11:4919. DOI PubMed PMC
140. Gui B, Liu X, Cheng Y, et al. Tailoring the pore surface of 3D covalent organic frameworks via post-synthetic click chemistry. *Angew Chem Int Ed Engl* 2022;61:e202113852. DOI
141. Wu Y, Weckhuysen BM. Separation and purification of hydrocarbons with porous materials. *Angew Chem Int Ed Engl* 2021;60:18930-49. DOI PubMed PMC
142. Baldwin LA, Crowe JW, Pyles DA, McGrier PL. Metalation of a mesoporous three-dimensional covalent organic framework. *J Am Chem Soc* 2016;138:15134-7. DOI PubMed
143. Jin F, Lin E, Wang T, et al. Bottom-up synthesis of 8-connected three-dimensional covalent organic frameworks for highly efficient ethylene/ethane separation. *J Am Chem Soc* 2022;144:5643-52. DOI
144. Gong C, Wang H, Sheng G, et al. Synthesis and visualization of entangled 3D covalent organic frameworks with high-valency stereoscopic molecular nodes for gas separation. *Angew Chem Int Ed Engl* 2022;61:e202204899. DOI
145. Li J, Zhou X, Wang J, Li X. Two-dimensional covalent organic frameworks (COFs) for membrane separation: a mini review. *Ind Eng Chem Res* 2019;58:15394-406. DOI
146. Ying Y, Yang Y, Ying W, Peng X. Two-dimensional materials for novel liquid separation membranes. *Nanotechnology* 2016;27:332001. DOI
147. Shi X, Zhang Z, Yin C, et al. Design of three-dimensional covalent organic framework membranes for fast and robust organic solvent nanofiltration. *Angew Chem Int Ed Engl* 2022;61:e202207559. DOI
148. Mohammed AK, Al Khoori AA, Addicoat MA, et al. Solvent-influenced fragmentations in free-standing three-dimensional covalent organic framework membranes for hydrophobicity switching. *Angew Chem Int Ed Engl* 2022;61:e202200905. DOI PubMed PMC
149. Ma Y, Wang Y, Li H, et al. Three-dimensional chemically stable covalent organic frameworks through hydrophobic engineering.

Angew Chem Int Ed Engl 2020;59:19633-8. DOI
150. Ahmed I, Jhung SH. Covalent organic framework-based materials: synthesis, modification, and application in environmental remediation. *Coord Chem Rev* 2021;441:213989. DOI
151. Wang X, Shi B, Yang H, et al. Assembling covalent organic framework membranes with superior ion exchange capacity. *Nat Commun* 2022;13:1020. DOI PubMed PMC
152. Sun W, Zhang L, Xiang Y, Ye N. Preliminary exploration of the dye/salt separation performance of 2D and 3D covalent organic frameworks/nylon 6 membranes prepared by layer-by-layer strategy. *Chem Eng Res Des* 2023;193:759-67. DOI
153. Shi X, Zhang Z, Fang S, Wang J, Zhang Y, Wang Y. Flexible and robust three-dimensional covalent organic framework membranes for precise separations under extreme conditions. *Nano Lett* 2021;21:8355-62. DOI
154. Shi X, Zhang Z, Wei M, et al. Three-dimensional covalent organic framework membranes: synthesis by oligomer interfacial ripening and application in precise separations. *Macromolecules* 2022;55:3259-66. DOI
155. Lu Y, Zhang H, Zhu Y, Marriott PJ, Wang H. Emerging homochiral porous materials for enantiomer separation. *Adv Funct Mater* 2021;31:2101335. DOI
156. Han X, Huang J, Yuan C, Liu Y, Cui Y. Chiral 3D covalent organic frameworks for high performance liquid chromatographic enantioseparation. *J Am Chem Soc* 2018;140:892-5. DOI
157. Holcroft JM, Hartlieb KJ, Moghadam PZ, et al. Carbohydrate-mediated purification of petrochemicals. *J Am Chem Soc* 2015;137:5706-19. DOI
158. Qian HL, Yang C, Yan XP. Layer-by-layer preparation of 3D covalent organic framework/silica composites for chromatographic separation of position isomers. *Chem Commun* 2018;54:11765-8. DOI
159. Qian HL, Wang ZH, Yang J, Yan XP. Building-block exchange synthesis of amino-based three-dimensional covalent organic frameworks for gas chromatographic separation of isomers. *Chem Commun* 2022;58:8133-6. DOI
160. Du ML, Yang C, Qian HL, Yan XP. Hydroxyl-functionalized three-dimensional covalent organic framework for selective and rapid extraction of organophosphorus pesticides. *J Chromatogr A* 2022;1673:463071. DOI PubMed
161. Liu X, Yang C, Qian H, Yan X. Three-dimensional nanoporous covalent organic framework-incorporated monolithic columns for high-performance liquid chromatography. *ACS Appl Nano Mater* 2021;4:5437-43. DOI
162. Wang ZH, Yang C, Liu T, Qian HL, Yan XP. Particle size regulation of single-crystalline covalent organic frameworks for high performance of gas chromatography. *Anal Chem* 2023;95:8145-9. DOI PubMed
163. Zong R, Wang X, Yin H, et al. Capillary coated with three-dimensional covalent organic frameworks for separation of fluoroquinolones by open-tubular capillary electrochromatography. *J Chromatogr A* 2021;1656:462549. DOI
164. Yin H, Zhen Z, Ning W, Zhang L, Xiang Y, Ye N. Three-dimensional fluorinated covalent organic frameworks coated capillary for the separation of fluoroquinolones by capillary electrochromatography. *J Chromatogr A* 2023;1706:464234. DOI
165. Niu X, Lv W, Sun Y, Dai H, Chen H, Chen X. In situ fabrication of 3D COF-300 in a capillary for separation of aromatic compounds by open-tubular capillary electrochromatography. *Mikrochim Acta* 2020;187:233. DOI
166. Guo J, Jiang D. Covalent organic frameworks for heterogeneous catalysis: principle, current status, and challenges. *ACS Cent Sci* 2020;6:869-79. DOI PubMed PMC
167. Zhi Y, Wang Z, Zhang HL, Zhang Q. Recent progress in metal-free covalent organic frameworks as heterogeneous catalysts. *Small* 2020;16:2001070. DOI
168. Zhang H, Lou LL, Yu K, Liu S. Advances in chiral metal-organic and covalent organic frameworks for asymmetric catalysis. *Small* 2021;17:e2005686. DOI PubMed
169. Xiao J, Liu X, Pan L, Shi C, Zhang X, Zou J. Heterogeneous photocatalytic organic transformation reactions using conjugated polymers-based materials. *ACS Catal* 2020;10:12256-83. DOI
170. Chen F, Guan X, Li H, et al. Three-dimensional radical covalent organic frameworks as highly efficient and stable catalysts for selective oxidation of alcohols. *Angew Chem Int Ed Engl* 2021;60:22230-5. DOI
171. Yan S, Guan X, Li H, et al. Three-dimensional salphen-based covalent-organic frameworks as catalytic antioxidants. *J Am Chem Soc* 2019;141:2920-4. DOI
172. Song J, Yu C, Liu Y, et al. An FeS*x* doped three-dimensional covalent organic framework for degradation of dyes. *Mater Chem Front* 2023;7:1431-6. DOI
173. Haque N, Biswas S, Ghosh S, Chowdhury AH, Khan A, Islam SM. Zn(II)-embedded nanoporous covalent organic frameworks for catalytic conversion of CO_2 under solvent-free conditions. *ACS Appl Nano Mater* 2021;4:7663-74. DOI
174. Liu Y, Wu C, Sun Q, et al. Spirobifluorene-based three-dimensional covalent organic frameworks with rigid topological channels as efficient heterogeneous catalyst. *CCS Chem* 2021;3:2418-27. DOI
175. Sun Q, Wu C, Pan Q, et al. Three-dimensional covalent-organic frameworks loaded with highly dispersed ultrafine palladium nanoparticles as efficient heterogeneous catalyst. *ChemNanoMat* 2021;7:95-9. DOI
176. Hou B, Yang S, Yang K, et al. Confinement-driven enantioselectivity in 3D porous chiral covalent organic frameworks. *Angew Chem Int Ed Engl* 2021;60:6086-93. DOI
177. Huang J, Tao Y, Ran S, et al. A hydroxy-containing three dimensional covalent organic framework bearing silver nanoparticles for reduction of 4-nitrophenol and degradation of organic dyes. *New J Chem* 2022;46:17153-60. DOI
178. Jin P, Niu X, Gao Z, et al. Ultrafine platinum nanoparticles supported on covalent organic frameworks as stable and reusable oxidase-like catalysts for cellular glutathione detection. *ACS Appl Nano Mater* 2021;4:5834-41. DOI

179. Ma YX, Li ZJ, Wei L, Ding SY, Zhang YB, Wang W. A dynamic three-dimensional covalent organic framework. *J Am Chem Soc* 2017;139:4995-8. DOI
180. Gao W, Sun X, Niu H, et al. Phosphomolybdic acid functionalized covalent organic frameworks: structure characterization and catalytic properties in olefin epoxidation. *Micropor Mesopor Mater* 2015;213:59-67. DOI
181. He T, Zhao Y. Covalent organic frameworks for energy conversion in photocatalysis. *Angew Chem Int Ed Engl* 2023;62:e202303086. DOI PubMed
182. Meng Y, Luo Y, Shi JL, et al. 2D and 3D porphyrinic covalent organic frameworks: the influence of dimensionality on functionality. *Angew Chem Int Ed Engl* 2020;59:3624-9. DOI
183. Chao J, Wang Z, Liu H, et al. A photo- and redox actives mesoporous 3D covalent organic framework enables highly efficient metal-free photoredox catalysis. *J Catal* 2022;413:692-702. DOI
184. Wang XL, Sun YY, Xiao Y, Chen XX, Huang XC, Zhou HL. Facile solution-refluxing synthesis and photocatalytic dye degradation of a dynamic covalent organic framework. *Molecules* 2022;27:8002. DOI PubMed PMC
185. Yu TY, Niu Q, Chen Y, et al. Interpenetrating 3D covalent organic framework for selective stilbene photoisomerization and photocyclization. *J Am Chem Soc* 2023;145:8860-70. DOI
186. Lu M, Zhang SB, Yang MY, et al. Dual photosensitizer coupled three-dimensional metal-covalent organic frameworks for efficient photocatalytic reactions. *Angew Chem Int Ed Engl* 2023;62:e202307632. DOI
187. Dong P, Xu X, Luo R, Yuan S, Zhou J, Lei J. Postsynthetic annulation of three-dimensional covalent organic frameworks for boosting CO_2 photoreduction. *J Am Chem Soc* 2023;145:15473-81. DOI PubMed
188. Lin G, Ding H, Chen R, Peng Z, Wang B, Wang C. 3D porphyrin-based covalent organic frameworks. *J Am Chem Soc* 2017;139:8705-9. DOI
189. Hynek J, Zelenka J, Rathouský J, et al. Designing porphyrinic covalent organic frameworks for the photodynamic inactivation of bacteria. *ACS Appl Mater Interfaces* 2018;10:8527-35. DOI
190. Zhang X, Wang S, Tang K, et al. Cu^{2+} embedded three-dimensional covalent organic framework for multiple ROS-based cancer immunotherapy. *ACS Appl Mater Interfaces* 2022;14:30618-25. DOI
191. Yan D, Lin E, Jin F, et al. Engineering COFs as smart triggers for rapid capture and controlled release of singlet oxygen. *J Mater Chem A* 2021;9:27434-41. DOI
192. Zhang L, Yang LL, Wan SC, et al. Three-dimensional covalent organic frameworks with cross-linked pores for efficient cancer immunotherapy. *Nano Lett* 2021;21:7979-88. DOI
193. Kim J, Kim H, Han GH, et al. Electrodeposition: an efficient method to fabricate self-supported electrodes for electrochemical energy conversion systems. *Exploration* 2022;2:20210077. DOI PubMed PMC
194. Li D, Li C, Zhang L, et al. Metal-free thiophene-sulfur covalent organic frameworks: precise and controllable synthesis of catalytic active sites for oxygen reduction. *J Am Chem Soc* 2020;142:8104-8. DOI
195. Liu J, Zhao J, Li C, et al. Precise modulation of carbon activity sites in metal-free covalent organic frameworks for enhanced oxygen reduction electrocatalysis. *Small* 2024;20:2305759. DOI
196. Li J, Jia J, Suo J, et al. Metal-free covalent organic frameworks containing precise heteroatoms for electrocatalytic oxygen reduction reaction. *J Mater Chem A* 2023;11:18349-55. DOI
197. Chang J, Li C, Wang X, et al. Quasi-three-dimensional cyclotriphosphazene-based covalent organic framework nanosheet for efficient oxygen reduction. *Nanomicro Lett* 2023;15:159. DOI PubMed PMC
198. Wang R, Zhang Z, Suo J, et al. Exploring metal-free ionic covalent organic framework nanosheets as efficient OER electrocatalysts via cationic-π interactions. *Chem Eng J* 2023;478:147403. DOI
199. Liu Y, Yan X, Li T, et al. Three-dimensional porphyrin-based covalent organic frameworks with tetrahedral building blocks for single-site catalysis. *New J Chem* 2019;43:16907-14. DOI
200. Gong C, Yang X, Wei X, et al. Three-dimensional porphyrin-based covalent organic frameworks with stp topology for an efficient electrocatalytic oxygen evolution reaction. *Mater Chem Front* 2023;7:230-7. DOI
201. Meng H, Wu B, Sun T, et al. Oxidization-induced structural optimization of Ni_3Fe-N-C derived from 3D covalent organic framework for high-efficiency and durable oxygen evolution reaction. *Nano Res* 2023;16:6710-20. DOI
202. Tavakoli E, Kakekhani A, Kaviani S, et al. In situ bottom-up synthesis of porphyrin-based covalent organic frameworks. *J Am Chem Soc* 2019;141:19560-4. DOI
203. Zhou M, Liu M, Miao Q, Shui H, Xu Q. Synergetic Pt atoms and nanoparticles anchored in standing carbon-derived from covalent organic frameworks for catalyzing ORR. *Adv Materials Inter* 2022;9:2201263. DOI
204. Li J, Liu P, Mao J, Yan J, Song W. Revealing the structure-activity relationship in woven covalent organic frameworks for the electrocatalytic oxygen reduction reaction. *Nanoscale* 2022;14:6126-32. DOI
205. Bao R, Xiang Z, Qiao Z, et al. Designing thiophene-enriched fully conjugated 3D covalent organic framework as metal-free oxygen reduction catalyst for hydrogen fuel cells. *Angew Chem Int Ed Engl* 2023;62:e202216751. DOI
206. Chi S, Chen Q, Zhao S, et al. Three-dimensional porphyrinic covalent organic frameworks for highly efficient electroreduction of carbon dioxide. *J Mater Chem A* 2022;10:4653-9. DOI
207. Han B, Jin Y, Chen B, et al. Maximizing electroactive sites in a three-dimensional covalent organic framework for significantly improved carbon dioxide reduction electrocatalysis. *Angew Chem Int Ed Engl* 2022;61:e202114244. DOI
208. Yusran Y, Fang Q, Valtchev V. Electroactive covalent organic frameworks: design, synthesis, and applications. *Adv Mater*

2020;32:e2002038. DOI

209. Li H, Chang J, Li S, et al. Three-dimensional tetrathiafulvalene-based covalent organic frameworks for tunable electrical conductivity. *J Am Chem Soc* 2019;141:13324-9. DOI
210. Li R, Xing G, Li H, Li S, Chen L. A three-dimensional polycyclic aromatic hydrocarbon based covalent organic framework doped with iodine for electrical conduction. *Chinese Chem Lett* 2023;34:107454. DOI
211. Wang S, Da L, Hao J, et al. A fully conjugated 3D covalent organic framework exhibiting band-like transport with ultrahigh electron mobility. *Angew Chem Int Ed Engl* 2021;60:9321-5. DOI
212. Yang Y, Mallick S, Izquierdo-Ruiz F, et al. A highly conductive all-carbon linked 3D covalent organic framework film. *Small* 2021;17:2103152. DOI
213. Zhao X, Chen Y, Wang Z, Zhang Z. Design and application of covalent organic frameworks for ionic conduction. *Polym Chem* 2021;12:4874-94. DOI
214. Wang S, Li X, Cheng T, et al. Highly conjugated three-dimensional covalent organic frameworks with enhanced Li-ion conductivity as solid-state electrolytes for high-performance lithium metal batteries. *J Mater Chem A* 2022;10:8761-71. DOI
215. Wu M, Huang H, Xu B, Zhang G. Poly(ethylene glycol)-functionalized 3D covalent organic frameworks as solid-state polyelectrolytes. *RSC Adv* 2022;12:16354-7. DOI PubMed PMC
216. Fan C, Geng H, Wu H, et al. Three-dimensional covalent organic framework membrane for efficient proton conduction. *J Mater Chem A* 2021;9:17720-3. DOI
217. Yu X, Li C, Chang J, et al. Gating effects for ion transport in three-dimensional functionalized covalent organic frameworks. *Angew Chem Int Ed Engl* 2022;61:e202200820. DOI
218. Sun J, Xu Y, Lv Y, Zhang Q, Zhou X. Recent advances in covalent organic framework electrode materials for alkali metal-ion batteries. *CCS Chem* 2023;5:1259-76. DOI
219. Yu X, Li C, Ma Y, et al. Crystalline, porous, covalent polyoxometalate-organic frameworks for lithium-ion batteries. *Micropor Mesopor Mater* 2020;299:110105. DOI
220. Schon TB, Tilley AJ, Kynaston EL, Seferos DS. Three-dimensional arylene diimide frameworks for highly stable lithium ion batteries. *ACS Appl Mater Interfaces* 2017;9:15631-7. DOI PubMed
221. Chen R, Zhao J, Yu Z, et al. Post-synthetic fully π-conjugated three-dimensional covalent organic frameworks for high-performance lithium storage. *ACS Appl Mater Interfaces* 2023;15:830-7. DOI
222. Wang Y, Li M, Wen T, Gu G. A 3D COF constructed by interlayer crosslinking of 2D COF as cathode material for lithium-sulfur batteries. *Nanotechnology* 2023;34:375402. DOI
223. Li Z, Zhou H, Zhao F, et al. Three-dimensional covalent organic frameworks as host materials for lithium-sulfur batteries. *Chin J Polym Sci* 2020;38:550-7. DOI
224. Liu W, Gong L, Liu Z, et al. Conjugated three-dimensional high-connected covalent organic frameworks for lithium-sulfur batteries. *J Am Chem Soc* 2022;144:17209-18. DOI
225. Wu K, Shi X, Yu F, et al. Molecularly engineered three-dimensional covalent organic framework protection films for highly stable zinc anodes in aqueous electrolyte. *Energy Storage Mater* 2022;51:391-9. DOI
226. Wu C, Liu Y, Liu H, et al. Highly conjugated three-dimensional covalent organic frameworks based on spirobifluorene for perovskite solar cell enhancement. *J Am Chem Soc* 2018;140:10016-24. DOI
227. Biradar MR, Rao CRK, Bhosale SV, Bhosale SV. Flame-retardant 3D covalent organic framework for high-performance symmetric supercapacitors. *Energy Fuels* 2023;37:4671-81. DOI
228. Chen S, Zhu C, Xian W, et al. Imparting ion selectivity to covalent organic framework membranes using de novo assembly for blue energy harvesting. *J Am Chem Soc* 2021;143:9415-22. DOI
229. Liu Y, Ren J, Wang Y, et al. A stable luminescent covalent organic framework nanosheet for sensitive molecular recognition. *CCS Chem* 2023;5:2033-45. DOI
230. Skorjanc T, Shetty D, Valant M. Covalent organic polymers and frameworks for fluorescence-based sensors. *ACS Sens* 2021;6:1461-81. DOI PubMed PMC
231. Ding H, Li J, Xie G, et al. An AIEgen-based 3D covalent organic framework for white light-emitting diodes. *Nat Commun* 2018;9:5234. DOI PubMed PMC
232. Cheng Y, Xin J, Xiao L, et al. A fluorescent three-dimensional covalent organic framework formed by the entanglement of two-dimensional sheets. *J Am Chem Soc* 2023;145:18737-41. DOI
233. Yuan Y, Ren H, Sun F, et al. Targeted synthesis of a 3D crystalline porous aromatic framework with luminescence quenching ability for hazardous and explosive molecules. *J Phys Chem C* 2012;116:26431-5. DOI
234. Li WK, Ren P, Zhou YW, Feng JT, Ma ZQ. Europium(III) functionalized 3D covalent organic framework for quinones adsorption and sensing investigation. *J Hazard Mater* 2020;388:121740. DOI PubMed
235. Wu M, Shan Z, Wang J, et al. Three-dimensional covalent organic frameworks based on a π-conjugated tetrahedral node. *Chem Commun* 2021;57:10379-82. DOI
236. Wang L, Chen Y, Zhang Z, Chen Y, Deng Q, Wang S. Bipyridine-linked three-dimensional covalent organic frameworks for fluorescence sensing of cobalt(II) at nanomole level. *Mikrochim Acta* 2021;188:167. DOI
237. Wei L, Sun T, Shi Z, et al. Guest-adaptive molecular sensing in a dynamic 3D covalent organic framework. *Nat Commun* 2022;13:7936. DOI PubMed PMC

238. Chi H, Wang L, Wang S, Liu G. An electrochemiluminescence sensor based on $CsPbBr_3$ -zquantum dots and poly (3-thiophene acetic acid) cross-linked nanogold imprinted layer for the determination of benzo(a)pyrene in edible oils. *Food Chem* 2023;426:136508. DOI
239. Zhao W, Yu C, Zhao J, et al. 3D hydrazone-functionalized covalent organic frameworks as pH-triggered rotary switches. *Small* 2021;17:2102630. DOI
240. Fang J, Fu Z, Chen X, et al. Piezochromism in dynamic three-dimensional covalent organic frameworks. *Angew Chem Int Ed Engl* 2023;62:e202304234. DOI
241. Liu X, Li J, Gui B, et al. A crystalline three-dimensional covalent organic framework with flexible building blocks. *J Am Chem Soc* 2021;143:2123-9. DOI
242. Dong X, Yang J, Wang H, et al. Synthesis of thin film of a three-dimensional covalent organic framework as anti-counterfeiting label. *Chin J Chem* 2022;40:1171-6. DOI
243. Bourda L, Kaczmarek AM, Peng M, et al. Turning 3D covalent organic frameworks into luminescent ratiometric temperature sensors. *ACS Appl Mater Interfaces* 2023;15:37696-705. DOI